Norwegian University of Life Sciences
Faculty of Veterinary Medicine and Biosciences
Department of Chemistry, Biotechnology and
Food Science

Master Thesis 2014
30 credits

The Influence of Divalent Metal Ions on a Lytic Polysaccharide Monooxygenase

Kaveh Naghshechi

ACKNOWLEDGMENTS

The present work was carried out at the Department of Chemistry, Biotechnology and Food Science at the Norwegian University of Life Sciences with Professor Vincent Eijsink and Dr. Gustav Vaaje-Kolstad as supervisors.

First of all, I would like to thank Vincent Eijink for giving me this opportunity to write my thesis in and be a part of the Protein Engineering and Proteomics (PEP) group. And I would specially thank Gustav Vaaje-Kolstad for ideas, inspiration and guidance throughout my work. And thank to all at the PEP group.

I would like to express my gratitude to my family and friends. Specially my better half who supported me all the way, thank you for all your support. To by little boy who probably did not understand why daddy had to sit behind the computer so much of the time. One day is you're turn Elia.

Thank you!

Drøbak 15 juni 201

Kaveh Naghshechi

ABSTRACT

Today's global environmental problems have brought focus to reaches filed working on finding new ways of generating energy without fossil use. In the field of biorefinery, enzymatic degradation of biomasses have had great focus, but still there it is a costly and slow process.

The recently discovered lytic polysaccharide monooxygenases (LPMO) members of the family auxiliary activity 10 (AA10) are have been showed to play an important role for degradation of insoluble polysaccharides. The discovery of the LPMOs have contributed to a greater understanding on how insoluble biomass in degraded in nature. This insight can be important for the future degradations techniques in this field. And reduce the demand for fossil fouls.

The gram-negative soil bacterium *Serratia marcescens* expresses the chitin-binding protein CBP21, a surface active LPMO AA-10 family. Previous studies have shown that CBP21 is a copper-metal dependent enzyme and additionally depends on an electron donor for enzyme activity. The aim of this study was to investigate the enzyme activity in the presence of other metal ions, this by a series of competitive inhibition assay where different divalent metal and, and ferric iron was added in various concentrations in reactions with CBP21, beta chitin and reductant. Reactions with different metals in different concentrations were analyzed qualitatively by MALDI-TOF MS and quantitative by UHPLS methods for detecting enzyme activity.

CBP21 showed activity in all solutions with the various metals up to 2 mM and 5 mM ion concentration except for in reaction with Fe^{3+}. Over time, there is no significant effect on CBP21 activity in reactions with Mn2 + or Ni2 +, but in reactions with Co2 + and Zn2 + were recorded partly inhibitory effect.

SAMMENDRAG

Med den globale miljøutfordringen som vi er stilt ovenfor i dag, har interessen og forskningen for bærekraftig og ren energi de siste tiårene vært fremtredende. Innenfor bioraffineri feltet har enzymatisk nedbrytning av biomasse vært i fokus, men er fortsatt en kostnadsfull og langsom prosess.

Nylig har det blitt vist at bakterielle enzymer kvalifisert som lytisk polysakkaride monooxygenase (LPMO) medlem av familien 10 av auxiliry activities (AA), øker nedbrytninghastigheten av uløselige polysakkarider. Disse oppdagelsene har bidratt til større kunnskap om mekanismen bak denne naturlige nedbrytningsprosessen, kunnskap som kan bli anvendes innen bioraffineriindustrien for en mer effektiv utnyttelse av biomasse og bidra til å redusere bruken av oljebaserte produkter.

Den gram negative jordbakterien *Serratia marcescens* uttrykker det kitin bindende proteinet CBP21, en overflate aktiv LPMO i AA-10 familien. Tidligere studier har vist at CBP21 er en kobber-metall avhengi enzym og i tillegg avhengi av en elektron donor ved enzym aktivitet. Målet for denne studien var å undersøke enzymets aktivitet i tilstedeværelse av andre metall ioner, dette ved en serie kompetitiv inhibering assay der ulike to-verdige mettall ioner, samt treverdig jern, ble tilført i ulike konsentrasjoner i reaksjoner med CBP21,beta-kitin og reduktant. Reaksjonene med ulike metaller i ulike konsentrasjoner ble analysert kvalitativ gjennom MALDI-TOF MS og kvantitativ ved UHPLS metoder for påvisning av enzym aktivitet.

CBP21 viste aktivitet i alle løsningene med de ulike metallene ved 2 mM og 5 mM ione konsentrasjon untatt for jern ionene. Over tid ble det ikke noe en signifikant effekt på CBP21 aktivitet i reaksjoner med Mn^{2+} eller Ni^{2+}, men i reaksjoner med Co^{2+} og Zn^{2+} ble det registrert dels inhiberende effekt.

ABRAVIATIONS

$CBP21_{wt}$	Copper saturated CBP21
CAZY	Carbohydrate-Active Enzymes
CBM	Carbohydrate Binding Module
CBM33	Carbohydrate Binding Module ofamily 33
CBP	Chitin Binding Protein
dH2O	Sterile water (Milli-Q)
EC	Enzyme Commission
g	Gravity
GH61	Glycoside hydrolase of family 61
GH	Glycosyl Hydrolase
GlcN	β-glucosamine
GlcNAc	N-acetyl-β-glucosamine
ITC	Isothermal titration calorimetry
kb	Kilobases
kDa	Kilo Dalton
LB	Luria Bertani
LPMo	Lytic Polysaccharide Monooxygenase
MALDI-TOF	Matrix-Assisted Laser Desorption Ionization -Time Of Flight
MS	Mass spectrometry spectrometry
OD	Optical density
rpm	Rotations per minute
SDS-PAGE	Sodium Dodecyl Sulphate PolyacrylAmide Gel Electrophoresis
UV	Ultraviolet
v/v	Volume/volume
w/v	Weight/volume
EDTA	Ethylenediaminetetraacetic acid
NMR	Nuclear magnetic resonance
UHPLC	Ultra high pressure liquid chromatography

AA	auxiliary activity

Contents

Today's global environmental problems have created the necessity for new energy sources from other than fossil fuels. Achieving an efficient and low coast method for enzymatic biomass conversion, can contribute to new energy sources, which is environmentally friendly and of economical importance. Especially the recently discovered lytic polysaccharide monooxygenases (LPMO) are likely to play an important role in future biorefinery. In this study the effect of metal ions on CBP21, a chitin-active LPMO from the Gram-negativs soil bacterium *Serratia marcescens* were explored, with the purpose of determining how CBP21 activity is affected in the presence of different metal ions.

1. INTRODUCTION

1.1 Polysaccharides

Carbohydrates are organic compounds with the general formula $C_x(H_2O)_y$, and are widely distributed in animals, plants and microorganisms. Carbohydrates are important biomolecules contributing too many functions in a cell e.g. maintaining structural integrity, use for energy storage and cell signaling. Monosaccharides are the basic units of all carbohydrates. When joined by glycosidic linkages, monosaccharides form polymeric chains. The glycosidic bond joining the monosacharides can either have an α− or β-conformation depending on the axial or equatorial orientation at the anomeric carbon (Figure 1.1). Depending on the degree of polymerization, such polymers are divided in three main groups: disaccharides, oligosaccharides and polysaccharides. More specifically, disaccharides consist of two monosaccharides, oligosaccharides are usually defined as carbohydrates made up of three to ten monosaccharides. Polysaccharides are defined by having more than ten linked monosaccharide residues, and there structures can range from linear to highly branched forms. Unlike other biopolymers (e.g polypeptides), polysaccharides rarely contain more than three different types of monosaccharide residues, and often only include one or two. (Harding & Adams, 2002)

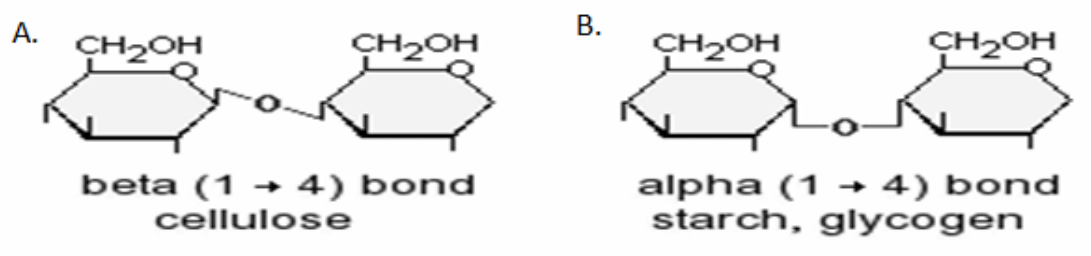

Figure 1.1. Glycosidic linkages. Glycosidic linkages can be in the β-conformation as in cellulose (A) or in the α-conformation, as in glycogen. Figure source: http://www.vivo.colostate.edu/hbooks/pathphys/digestion/basics/foodchem.html

Two of the most abundant forms of polysaccharides in nature are the linear polymers cellulose and chitin. These two polysaccharides are important structural biomolecules and form an unsolvable unsalable crystalline structure giving the organism a robust biological structure (Gooday, 1990).

1.1.2 Chitin

Chitin is the second most abundant biopolymer in the biosphere next to cellulose. It's a linear homo polymer of ß(1-4) linked N-acetyl-D-glucosamine (GlcNAc) units, where the monosaccharides are rotated 180^{o} relative to each other. and (figure 1.2) (Rinaudo, 2006) .The global production of chitin is estimated to be around 10^{10}-10^{11} tons each year. Chitin is an insoluble polymer and is organized in crystalline nanofibrils. The chitin structure is rigid and can endure mechanic and chemical stress. In nature, chitin is exploited by many organisms to maintain structural integrity e.g. in the exoskeletons of arthropods, insects and in the cell walls of fungi (Gooday, 1990)

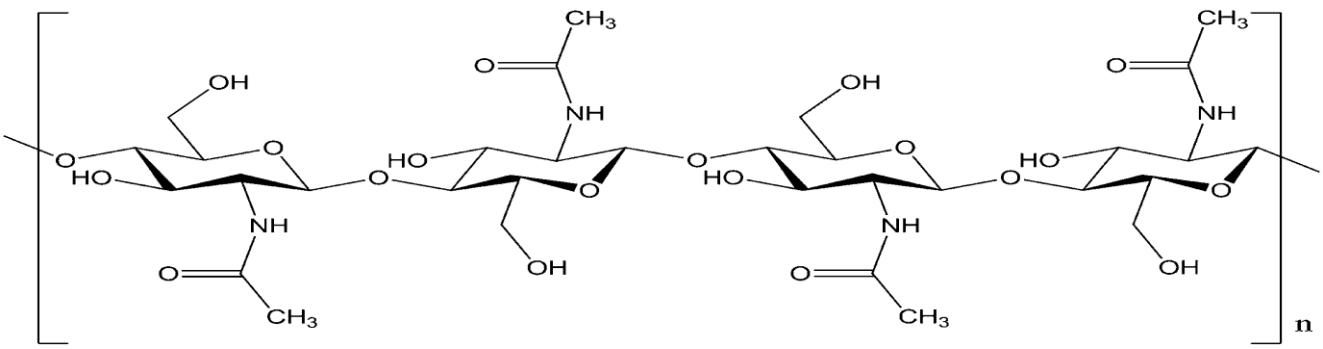

Figure 1.2. The structure of chitin. Chitin consists of repeating units of disaccharides with subsequent monomers of ß(1-4) linked N-acetyl-D-glucosamine. Figure source - http://pubs.rsc.org/en/content/articlehtml/2014/gc/c3gc42436g

Chitin exists in three polymorphic forms, defined by the orientation of the polymer chains in the crystalline structure: α-chitin is characterized by anti-parallel chains, whereas in β-chitin the chains are organized in a parallel fashion. The third minor form, ɣ-chitin, has both parallel and anti-parallel chains. (Gardner & Blackwell, 1975; Minke & Blackwell, 1978).The polymer chains are stabilized by intermolecular hydrogen bonds, involving hydroxyl, amino and carbonyl groups, and leading to the formation of the micro fibrils (Carlström, 1957). The α-form is the most rigid and abundant form of chitin, stabilized by the large number of intermolecular hydrogen bonds (Giraud-Guille & Bouligand, 1986). It can found in the tough exoskeletons of arthropods. The β –form has fewer intramolecular hydrogen bonds which leads to a less stable structure (Jang, Kong, Jeong, Lee, & Nah, 2004). This β-form of chitin can be found in squid pen (Rudall & Kenchington, 1973).

1.2 Classification of carbohydrate active enzymes

The Enzyme Commission (EC) numbers provided by the Nomenclature Committee of the International Union of Biochemistry and Molecular Biology (IUBMB), correlates enzymes with the type of reaction they catalyze and their substrates specificity. In this database different enzymes that catalyze the same chemical reaction will receive the same EC-number. The system in consequence becomes problematic when enzymes are active against several substrates and the classification does not take into account protein sequence similarity or structural similarity (Hoell, Vaaje-Kolstad, & Eijsink, 2010). This problem was addressed when the carbohydrate-active enzyme database (CAZy) was established (http://www.cazy.org). CAZy describes families of structurally related catalytic and carbohydrate binding modules of enzymes that degrade, modify, or create glycosidic bonds (http://www.cazy.org). Enzymes belonging to this category are referred to as CAZymes. The CAZy database has been online since 1998 and is based on amino acid sequence similarities, protein folds and enzymatic mechanisms. The CAZy classification system reflects enzyme structure and mechanisms more than enzyme specificity, making the database a powerful tool for characterizing proteins with unknown function but known sequence (Cantarel et al., 2009). The enzyme classes currently covered by the CAZy database are: glycoside hydrolases (GH), polysaccharide lyases (PL), carbohydrate esterases (CE), glycosyltransferases (GT) and the newly added class of auxiliary activities (AAs). As of mars 2014, 133 families of GHs, 95

families of GT, 23 families of PLs, 16 families of CE and 11 families of AA are listed in the CAZy database (http://www.cazy.org/)

1.2.1 Chitin degradation

As already noted, chitin is one of the most abundant polymers in nature. Still there is no quantitatively significant long-term accumulation of chitin in the biosphere, implying efficient degradation and turnover (Tracey, 1957; Gooday, 1990a). It is thought that bacteria are the main mediators of chitin degradation, but chitin.degrading enzymes are also found in other organisms such as fungi (Gooday, 1990a). More specifically, the degradation of chitin is primarily done via two major pathways. One pathway involves the deacetylation of chitin to chitosan (Figure 1.3) by enzymes named deacetylases (EC 3.5.1.41, belonging to family 4 of the carbohydrate esterases), followed by hydrolysis of the (1-4)-β- glycosidic bonds in chitosan by chitosanases (EC 3.2.1.132, belonging to GH families 5, 7, 8, 46, 75 and 80-glycoside hydrolases) (Hoell et al., 2010).

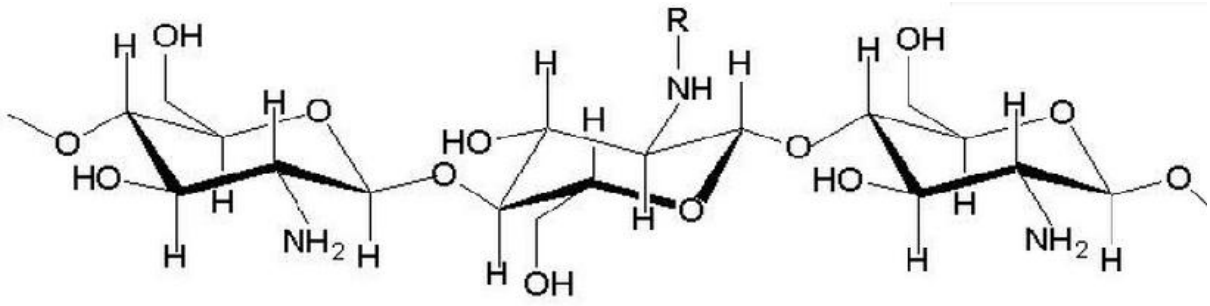

Figure 1.3 Chemical structure of chitosan. Chemical or enzymatic elimination of acetyl groups in the acetamido group converts chitin to chitosan. Figure source http://www.mn.uio.no/kjemi/english/people/aca/bony/research/chitosan.html

The second pathway is the chitinolytic, which is performed by the synergy of hydrolytic exo- and endo-acting chitinases. Chitinases (EC 3.2.1.14), which belong to glycoside hydrolase families 18 and 19, perform the initial hydrolysis of the (1-4)-β-glycosidic linkages in chitin. The initial hydrolysis results in dimers of GlcNAc that are subsequently degraded to monomers by chitobiases belonging to family 20 of the glycoside hydrolases (EC 3.2.1.29 (S. J. Horn et al., 2006). The chitinolytic pathway also contains an enzymatic contribution by the recently discovered lytic polysaccharide monooxygenases (LPMOs) that belong to family 9, 10 and 11 of the auxiliary activities. This enzyme activity cleaves glycosidic bonds in

crystalline chitin by an oxidative mechanism, which leads to increased substrate accessibility for chitinases and thereby boosts the hydrolysis of chitin (Vaaje-Kolstad et al., 2010). Understanding the mechanisms of chitin degradation can also contribute to understanding the degradation of other recalcitrant polymers in nature such as cellulose, which is structurally similar to chitin. This knowledge can in turn be utilized to generate an efficient pathway for production of second generation of biofuels (Eijsink, Vaaje-Kolstad, Vårum, & Horn, 2008).

1.3 Lytic Polysaccharide Monooxygenases LPMO

It has recently been discovered that members of carbohydrate-binding module family 33 (CBM33) and family GH61 are lytic polysaccharide monooxygenases (LPMOs). As of 2013, the CBM33 and GH61 families are classified as family 10 and 9 of the auxiliary activities (AA) in the CAZy database, respectively. Family AA9 and AA10 both use an oxidative mechanism to cleave crystalline polysaccharides such as chitin and cellulose (Levasseur, Drula, Lombard, Coutinho, & Henrissat, 2013). Proteins in the AA10 family are found in all domains of life, such as viruses, bacteria and fungi, whereas AA9 type enzymes are only present in fungi(Svein Jarle Horn, Vaaje-Kolstad, Westereng, & Eijsink, 2012; Suzuki, Suzuki, Taiyoji, Nikaidou, & Watanabe, 1998). Most of the LPMO-containing organisms encode several LPMOs that are unregulated when chitin or cellulose are their carbon source, indicating that these enzymes are important for the organism's ability to degrade biomass(Harris et al., 2010; Suzuki et al., 1998). The main focus of the research described here is the single domain chitin- active protein CBP21, which is an AA10 LPMO.

In 2005 Vaaje-Kolstad et al discovered that a protein called CBP21 increased the efficiency of chitinase degradation of crystalline chitin. In 2010 Vaaje- Kolstad et al showed that CBP21 is a metal-dependent enzyme that acts on the surface of crystalline chitin and break glycosidic bonds, and released oxidized products(Vaaje-Kolstad et al., 2010). CBP21 was the first LPMO which had its structure determined and is produced by the chitinolytic bacterium *Serratia marcescens*. The enzyme depolymerizes and disrupts the substrate making the

inaccessible polysaccharide material available for further degradation by chitinases(Vaaje-Kolstad et al., 2010).

In 2010 Harries et al studies showed the formation of oxidized sugar by GH61(further referred to as AA9), with cellulose as substrate, suggesting that AA9 activity is similar to AA10 enzymes . The two families; AA9 and AA10 shows no specific sequence identity less than 10% but they share structural similarities, and they have a conserved metal binding site in their catalytic center (Hemsworth et al., 2013), and they both have a flat substrate-bindig surface and unlike GH they require a divalent metal for optimal activity(Harris et al., 2010). Its taught that the flat substrate binding surface makes the enzymes unable to bind to soluble substrates, and that they are more optimized for binding at surfaces of complex insoluble structures (Vaaje-Kolstad et al., 2010; Westereng et al., 2011).

The AA9 and AA10 LPMOs have a similar highly conserved N-terminal histidine that together with a second conserved histidine coordinates a divalent matal ion in what is called a histidine brace. After some initial confusin this divalent metal ion was showed to be copper (Aachmann, Sorlie, Skjak-Braek, Eijsink, & Vaaje-Kolstad, 2012). The importance of the matal ion for this two enzymes have been investigated by binding-site mutation and adition of ethylenediaminetetraacetic acid (EDTA) wich led to reduced activity(Forsberg et al., 2011; Phillips, Beeson, Cate, & Marletta, 2011) but the detailed mechanism of this remain unrevealed. Philliph et al have proposed a mechanisem (Figure 1.4)

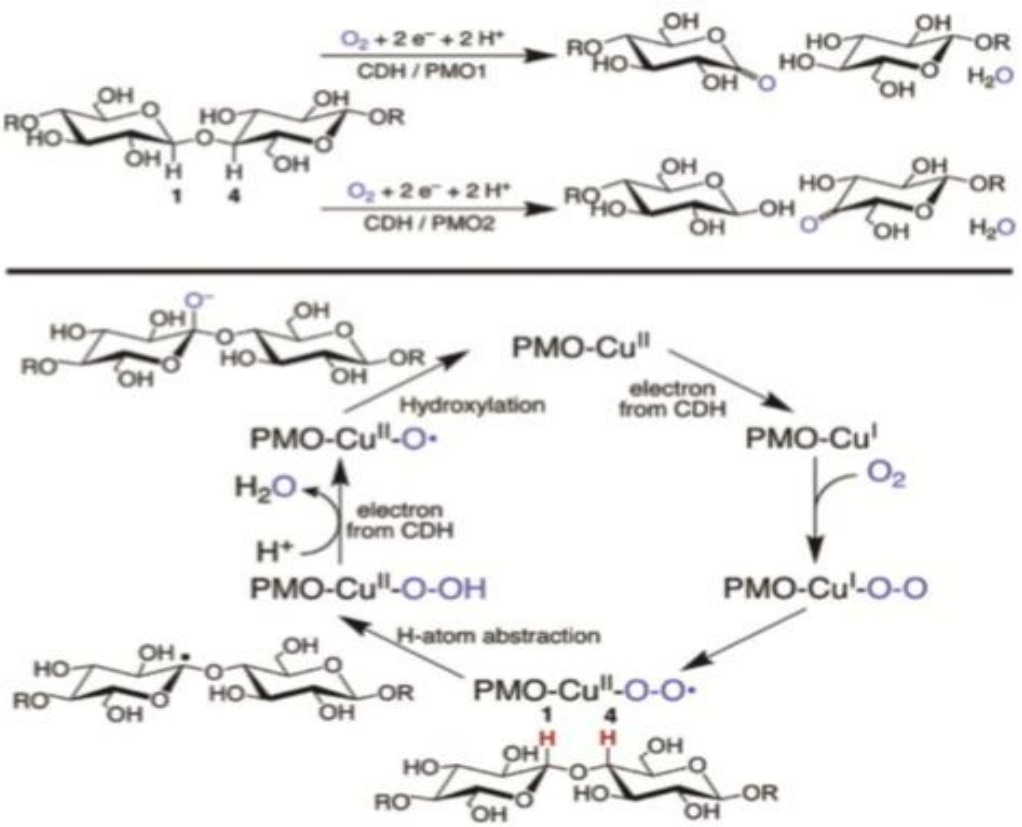

Figure 1.4 LPMO proposed reaction mechanism. (Top) Type 1 LPMO abstract a hydrogen atom from C1 leading to formation of a sugar lactones that further spontaneously hydrolyse to aldonic acid. Type 2 LMPO catalyze hydrogen atom abstraction from C4 leading to formation of ketoaldoses. Bottom LPMO mechanism: a electrone from the heme domain of CDH- reduces LPMO PMO Cu(II) to Cu(I) and then O2 binds. From internal electron transfer takes place to form a copper superoxo intermediate, which then abstracts a H• from the C 4 position on the carbohydrate. A second electron from CDH leads to homolytic cleavage of the Cu-bound hydroperoxide. The copper oxo species (Cu−O•) then couples with the substrate radical, hydroxylating the substrate. Addition of the oxygen atom destabilizes the glycosidic bond and leads to elimination of the adjacent glucan. (Phillips et al., 2011) this figure is from Philips et al. (2011)

1.4 The chitiolytic machinery of Serratia marcescens

Serratia marcescens, a gram negative soil bacterium classified as a member of the Enterobactericeae, has an efficient enzymatic machinery for degradation of chitin and is one of the most extensively studied chitinolytic bacteria (Monreal & Reese, 1969). Besides from being important for the degradation of polysaccharides in nature, *S. marcescens* has also been identified as a cause for nosocomial infections. The bacteria also produce a characteristic red pigment, prodigiosin (2-methyl-3-amyl-methoxypro-digiosene) which can be useful for

identification (Hejazi & Falkiner, 1997; Suzuki et al., 1998). *S. marcescens* produces three family 18 chitinases (ChiA, ChiB and ChiC) and a family 20 chitobiase when growing on chitin. The chitinolytic enzymes produced by *S. marcescens* play different roles in the conversion of the insoluble chitin-polymer. ChiA and ChiB are exo-acting processive chitinases attacking the chitin chains from opposite directions, whereas ChiC is an endo-acting non-processive chitinase cleaving the chitin chains at random positions in the chain. The chitinases perform the hydrolysis of the (1-4)-β-glycosidic linkages in chitin, which results in production of GlcNAc dimers that are subsequently degraded to monomers by the chitobiase. (Vaaje-Kolstad, Horn, van Aalten, Synstad, & Eijsink, 2005; Vaaje-Kolstad et al., 2010). In addition to the three chitinases and the chitobiase, the bacterium secretes the 18.8 kDa chitin-binding protein, CBP21, which is the main focus of this study. CBP21 is an LPMO that belongs to family AA10 and binds specifically to β-chitin (Suzuki et al. 1998), and has been shown to be especially important for chitinolysis by *S. marcescens*. CBP21 cleaves glycosidic bonds in crystalline chitin, increasing substrate accessibility for chitinases and provides new attachment sites for the processive enzymes, increasing the overall degradation of chitin by the chitinases (Figure 1.5) (Horn et al. 2006; Vaaje-Kolstad et al. 2010; Vaaje Kolstad et al. 2013).

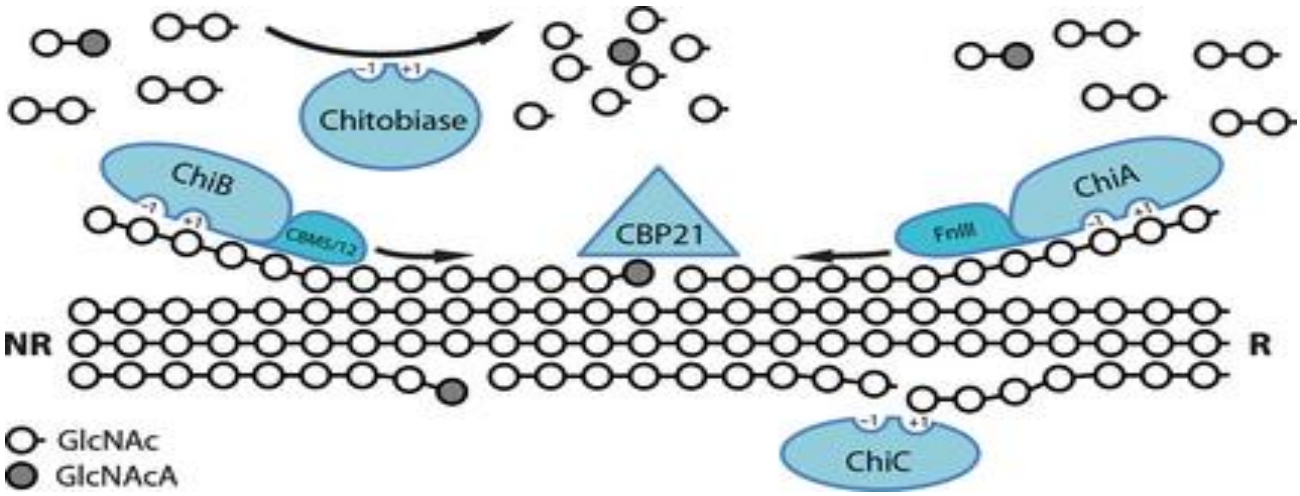

Figure 1.5. Overview of the chitinolytic machinery of *S. marcescens.* The figure shows how the chitin chain (open circles) is degraded. ChiA degrades the chain from the reducing end (R) and ChiB degrades the chain from the non reducing end (NR). ChiC randomly cleaves the more amorphous regions of the substrate, making the substrate more accessible for ChiA and ChiB. ChiC also has a CBM but the position is not known due do the lack of structural information. CBP21 cleaves the glycosidic bonds by an oxidative mechanism, increasing substrate accessibility for the chitinases (oxidized chain ends are marked grey). The chitobiase further degrades the products from chitinase activity (mostly chitobiose) to GlcNAc monomers.(Vaaje-Kolstad, Horn, Sorlie, & Eijsink, 2013). The figure is from Vaaje-Kolstad et al. (2013).

1.5 Chitin-binding protein 21, a family AA10 lytic polysaccharide monooxygenase

In 1986 Fuchs et al. showed that *S. marcescens* produces at least five different chitinolytic proteins, one of them being a 21 kDa protein now known as CBP21(Fuchs, McPherson, & Drahos, 1986). Further, in 1997, Watanabe et al. preformed an analysis of the chitinolytic machinery of *S. marcescens* 2170, which showed that the same 21 kDa protein (CBP21) exhibited chitin binding activity, but lacked chitinase activity. At this time it was postulated, based on the chitin binding activity and the production of CBP21 in presence of colloidal chitin, that CBP21 played a role in the degradation of chitin by the bacterium (Watanabe et al., 1997). A study aimed at providing greater knowledge of CBP21 by Suzuki et al. in 1998 revealed that the gene encoding CBP21 was located in a region 1.5 kb downstream of the *chiB* gene (sett inn referansen her). The *cbp* gene encodes a 197 amino acid polypeptide of 21.6 kDa in size, containing an N-terminal (Met-1 to Ala-27) signal sequence. The mature protein was calculated to be 18.8 kDa, and demonstrated highest binding affinity towards β-chitin.

Determination of the structure of CBP21 showed that the fold of CBP21 is most similar to a fibronectin type III (FnIII) domain, a frequent fold in eukaryotic proteins, which in bacteria has only been found among carbohydrate active enzymes.(Jee et al., 2002; Vaaje-Kolstad, Houston, Riemen, Eijsink, & van Aalten, 2005)

Early studies suggested that CBP21 increased chitinase activity by disturbing the crystalline structure of the substrate, hence making it more accessible for chitinases (Vaaje-Kolstad, Horn, et al., 2005). In 2010, Vaaje-Kolstad et al. demonstrated that CBP21 in fact is a metal-dependent enzyme, which makes the crystalline chitin available for degradation by chitinases, by depolymerization of the substrate using an oxidative mechanism (Vaaje-Kolstad et al., 2010). The fact that most chitin-degrading microorganisms contain homologues of CBP21, suggest a general mechanism where auxiliary chitin-binding proteins, now known to be LPMOs, enhance chitonolytic activity (Vaaje-Kolstad, Horn, et al., 2005). Knowledge of this type of enzymes can help understanding the mechanism behind degradation of polysaccharides, and is of great interest for the conversion of recalcitrant biomass to biofuels.

1.5.1 Structure of CBP21

The crystal structure of CBP21 (Figure 1.6) was the first structure of a family AA10 LPMO to be solved. The structure exhibited a three-stranded and a four-stranded β-sheet forming a β-sandwich, and a 65 residue pseudo domain containing three α-helices, a short α-helix and two short 3_{10} helices, located between β-sheet one and two. This 65 residue bud-like-pseudo domain is characteristic for theAA10 family. There are four cysteine residues forming two disulfide bridges, one in the pseudo-domain and the second between β-sheet fire and five. (Vaaje-Kolstad, Houston, et al., 2005). Previous studies have demonstrated that enzymes which display affinity for carbohydrates contain substrate binding clefts or tunnel, with a patch of aromatic residues extending over the surface of the binding area (Perrakis et al., 1994). In the case of CBP21 conserved aromatic residues such as Trp-94, Trp-108, Trp-119, Tyr-121, Trp-128, Trp-178, Phe-187, and Tyr-188 are buried in the hydrophobic core of the protein. The flat surface containing additional conserved residues mainly shows solvent-exposed polar side chains, except from Tyr-54 which is an aromatic residue (Vaaje-Kolstad, Horn, et al., 2005). The N-terminal histidine (His-28) and His114 show a high degree of conservation and their imidazole side chain moieties and the amino terminus of His28 constitute a copper binding site (Aachmann et al., 2012; Vaaje-Kolstad et al., 2010). The cluster of mainly hydrophilic residues on the CBP21 surface has been subjected for mutational experiments, with the intention of revealing their role in substrate binding. These studies showed thatindividual mutationsof Tyr-54, Glu-55, Glu-66, His-114, Asp-182, and Asn-185 to alanine, all showed decreased chitin affinity. The highest increase in dissociation constant (K_d) (decrease chitin affinity) was found for mutants Y54A and E60A. Notably all mutants demonstrated a certain degree of chitin affinity, indicating that a larger cluster of conserved residues on the surface of the enzyme is important for substrate binding. Hydrolysis of β-chitin with ChiC and CBP21 mutants (Y54A, E55A, E60A, H114A, D182A and N185) demonstrated that all mutants except N185A have abolished ability to assist chitin turnover by ChiC. Mutant N185A showed reduced chitin affinity, but was still able to increase chitin turnover by ChiC, suggesting that N185 is promoting ligand binding only, while the other residues (Y54, E55, E60, H114 and D182) are more involved in the chitin

depolymerization (Vaaje-Kolstad, Horn, et al., 2005).

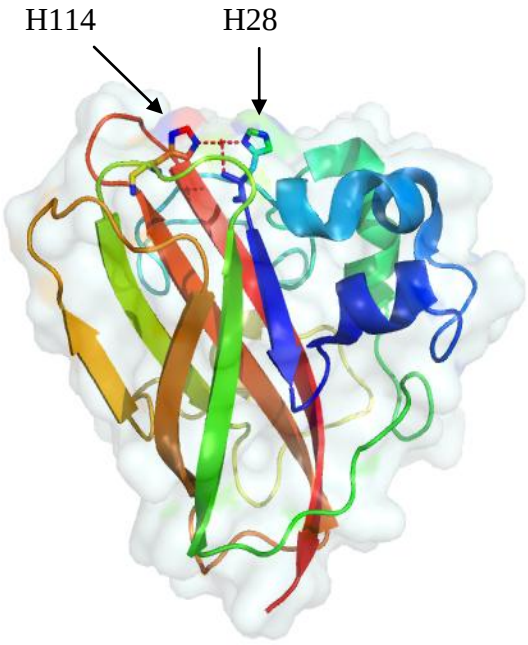

Figure 1.6. Crystal structure of CBP21. (Uniprot ID: O83009; PDB ID: 2BEM) CBP21 from *Serratia marcescens*. His 28 and His114, responsible for the copper binding, are marked on the picture. This figure was generated using PyMOL

1.5.2 The copper binding site of CBP21

In 2012 Aachmann et al. did a study using NMR and ITC techniques to revel structural and functional aspects of CBP21. Interactions of CBP21 with divalent metal ions was probed by recording changes in the chemical shift in ^{15}N hetero- nuclear single quantum coherence (HSQC) spectra upon titration with $Ca^{2+,}$ Mg 2+, Fe^{3+} , $Co^{2+,}$, $Zn^{2+,}$, or $Cu^{2+,}$ ions. All metal ions showed binding to the interaction site located between His28 and His114(Figure 1.7), where the side chain in both residues and the N-terminal amino group of His 28 coordinate the metal ion (Aachmann et al., 2012)

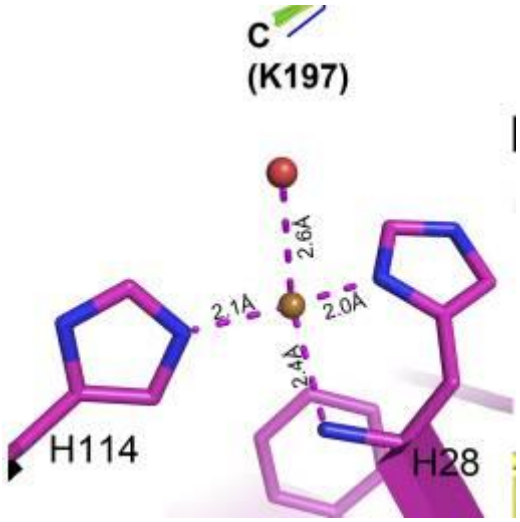

Figure 1.7 Metal binding site of CBP21. Showing the N-terminal His28 and His114 coordinating the metal ion. The picture is from Aachmann et al. 2012.

Experiment estimated the dissociation constant(Kd) for each of the metals to have the following order $Ca^{2+} > Mg^{2+} > Fe^{2+} > Co^{2+} >> Zn^{3+} > Cu^{2+}$. And further ITC method was used to obtain accurate date for the dissociation constant for Zn^{2+} and Cu^{2+}, which was determent to be 330 and 55 nM, respectively, showing that Cu^{2+} bind almost six time more tightly than Zn^{2+}.(Aachmann et al., 2012). This data revels that the CBP21 is a Copper dependent LMPO, and that Cu^{2+} binding to the enzyme is essential for catalysis. They also showed that Cu^{1+} reflected tighter binding relative to the Cu^{2+} ion (Aachmann et al., 2012). The fact that several ions are able to bind to the interaction site makes it interesting to explore the effects from other metal ion of CBP21 activity.

1.5.3 Catalysis by CBP21, a family AA 10 LPMO

In 2010, an eminent study from Vaaje kolstad et al. contributed to essential knowledge on the enzymatic activity of CBP21. The authors showed that CBP21 is a metal dependent enzyme that cleaves chitin in presence of external electrone donor and molecular oxygen. Enzymatic activity was discovered upon detection of soluble products released from chitin mediated by CBP21 activity. The products turned out to be chitin oligosaccharides with a native GlcNAc at the non-reducing end and an oxidized GlcNAc, 2-(acetylamino)-2-deoxy-D-gluconic acid at the downstream end (Vaaje-Kolstad et al., 2010). The majority of the visible soluble products generated by CBP21 had a degree of polymerization beneath 10 and a clear

dominance of even number oligomers (Vaaje-Kolstad et al., 2010). Product with higher DP will probably stay bound to the remaining insoluble chitin and are unable to be detected. The dominance of even numbered products was interpreted to be a result of CBP21 acting on the flat crystalline surface of the chitin microfibrils. Due to chitobiose being the repeating unit of the chitin chain the enzyme can only bind productively regions on a chain that is separated by an even number of GlcNAc residues. Experiments with isotope-labeled reactants ($H_2{}^{18}O$ and $^{18}O_2$) were conducted trying to reveal the CBP21 mechanism. From these experiments it was concluded that the oxidized product, contained one oxygen coming from O_2 and one from H_2O (Figure 1.7). Further the need for molecular oxygen was confirmed when experiment revealed that activity was significantly inhibited by cyanide, a known O_2 mimic.(Vaaje-Kolstad et al., 2013; Vaaje-Kolstad et al., 2010). The incorporation of the H_2O most likely occurs after cleavage of the glycosidic bond since it is likely that the product generated by the oxidation is a 1,5-δ-lactone. After being released into solution, which is at physiological pH, the lactone will spontaneously hydrolyze, thereby forming the gluconic acid (Figure 1.7)(at acidic Ph the equilibrium is driven towards the lactone form). The enzymatic action of CBP21on chitin produces negatively charged aldonic acids, this aldonic acid have no longer the cyclic hexose conformation, suggesting that it becomes more prone for degradation by other enzymes in the chitiolytic pathway (Vaaje-Kolstad et al., 2010).

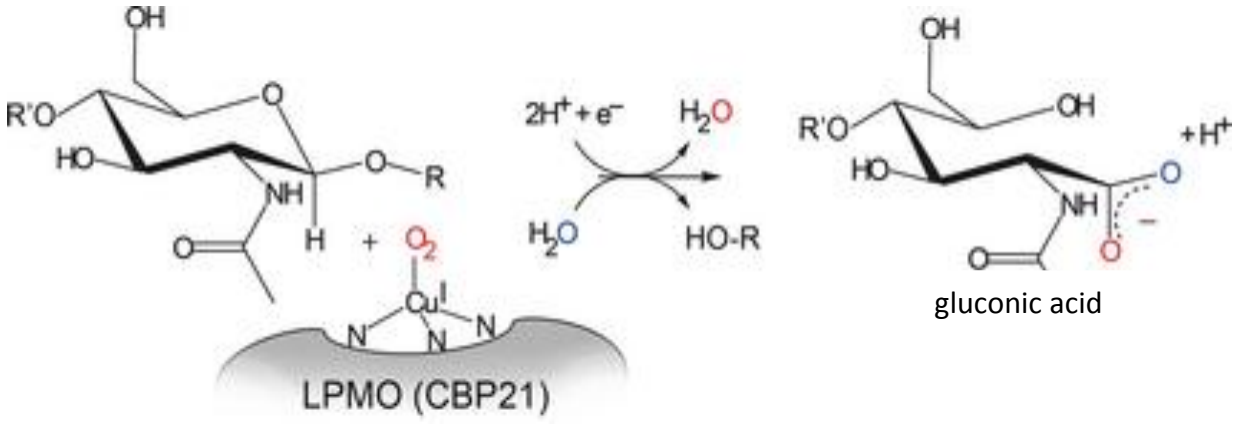

Figure 1.8 Scheme for the reaction catalysed by CBP21. The copper (Cu^{2+}) ion is reduced to Cu^{+} on the enzyme by an external reductant , this increase the affinity for molecular oxygen. The reduced copper is responsible for transferring electron to molecular oxygen. The enzyme now attached to O2 carries out a cleavage which the mechanism is not fully understood. The action of CBP21 generates two products, one non-oxidized product (HO-R) and one aldonic acid with an oxidized end. The oxidized product containing oxygen coming from O2 marked red, and one oxygen resulting from the hydrolysis by bulk water (marked in blue). The figure is from Vaaje-kolstad et al. 2013.

Additional experiments also showed that metal ion chelator (EDTA) led to inactivation of CBP21, indicating that the enzyme is metal dependent (section 1.4.2 for detailed binding site description). While, initially, the identity of the metal ion was somewhat unclear (Harris et al., 2010; Vaaje-Kolstad et al., 2010), it has later been showed that LPMOs in the AA10 family are in fact copper dependent (Hemsworth et al., 2013; Vaaje-Kolstad et al., 2010) Vaaje-Kolstad et al further explored the necessity of an electron donor. Indeed it was demonstrated that the oxidation step depends on an external electron donor, reflected in a large increase in activity in presence of reductans such as ascorbic acid, reduced gluathione or Fe(II)SO4, (Vaaje-Kolstad et al., 2010).

1.6 Purpose of study

Gaining a greater understanding of the machinery behind degradation of insoluble polysaccharides such as cellulose and chitin, are important for the improvement of industrial techniques where biomass is enzymatic converted to easily fermentable compounds. The goal for this study is to explore how the enzymatic activity of CBP21, a metal dependent lytical polysaccharide monooxyganese from family AA10, is affected in presence of a variety of metal ions. Considering the dominance of LPMOs in the secretoms of biomass degrading microorganism and the documented effect of LPMOs on biomass conversion, indicates that this are very important enzymes and that they can be a of great contribution in development of enzymatich pathways for biomass refining.

Data on how the enzymatic capability of CBP21 is affected in presence of such metal ions, can contribute to a change how the substrate (chitin) is treated previous to degradation. Such as if decontamination of metals ions prior to degradation is needed. There are also strong indications that similar enzyme exits that works on cellulose, making the insight of CBP21 mechanism adaptable toward enzyme degradation cellulose and other polysaccharides.

To achieve this goal, a competition experiments where varieties of metals were incubated with $CBP21_{wt}$ at different concentrations was conducted. Methods such as MALDI-TOF and UHPLC were performed to qualitatively and quantitatively analyze the effect from the metal ions on $CBP21_{wt}$ activity.

2. MATERIAL AND CHEMICALES

2.1 Chemicals

Chemical	Supplier
3-Hydroxyanthranilic acid	Sigma-Aldrich
2,5-Dihydroxybenzoic acid (DHB)	Bruker Daltonics
Agar bacteriological (Agar No. 1)	Oxoid
Agarose, SeaKem®	Lonza
Acetic acid, CH_3CO_2H	VWR
Acetonitrile, CH_3CN	VWR
Ammonium sulphate, $NaSO_4$	Merck
Ampicillin	Sigma-Aldrich
Bacto™ yeast extract	Becton, Dickinson and co
Bacto™ trypton	Becton, Dickinson and co
Bis-Tris	Sigma-Aldrich
Copper sulphate, $Cu(II)SO_4$	Sigma-Aldrich
Nikkel sulphate, $Ni(II)SO_4$	Sigma-Aldrich
$Fe(III)\ SO_4$	Sigma-Aldrich
Manganese sulphate $Mn(II)SO_4$	Sigma-Aldrich
Zink sulphate $Zn(II)SO_4$	Sigma-Aldrich
Cobalt sulphate $Co(II)SO_4$	Sigma-Aldrich
Sodium hydroxide, NaOH	Sigma-Aldrich
Sulphuric acid, H_2SO_4	Sigma-Aldrich
Sodium chloride, NaCl	J.T. Baker
Coomassie Brilliant Blue R250	Merck
Ethanol, 96 % (w/v)	Arcus
Ethylenediaminetetraacetic acid (EDTA)	Sigma-Aldrich
Glycerol, 85 % (w/v)	Merck

Hydrochloric acid, HCl	Merck
L -Ascorbic acid	Sigma-Aldrich
Magnesium chloride, $MgCl_2$	Qiagen
Methanol, 85 % (w/v)	Merck
Phenylmethanesulfonylfluoride (PMSF)	Sigma-Aldrich
Chelex® 100 sodium form	Sigma-Aldrich

2.2 Laboratory instruments

Instrument	**Brand**
BioLogic LP chromatographic system	BioRad
Avanti™ J-25 centrifuge with JA-14 rotor	Beckman Coulter
Centrifuge, 5418 R	Eppendorf
Centrifuge, 5430 R	Eppendorf
MALDI-TOF MS, Ultra flex instrument	Bruker Daltonics
Thermo Scientific Open Heating Bath Circulator, ED-7A/B	Julabo
pH meter 827	Metrohm
Power Pac 300 power supply	BioRad
Rotary shaker, IKA ® HS 260 basic	Bie & Berntsen Semi
Hitachi Thermomixer, Comfort	Eppendorf
Thermomixer, Vortemp	Thermo Scientific High
Output Vacuum pump	Millipore
Gel doc™ EZ imager	BioRad
Biophotometer™	Eppendorf
MultiScreenHTS Vacuum Manifold	Millipore
Agilent 1290 Infinity LC system	GE Healthcare
Phenomene Dionex Ultimate 3000 RSLC HPLC	Ultimate

2.3 Family AA 10 and plasmids

Protein	Strain	Plasmid	Reference
CBP21	*Serratia marcescens* BJL 200	pRSET-B/cbp21	(Vaaje-Kolstad, Horn, et al., 2005)

2.4 Bacterial strain

Strain	Application	supplier
Escherichia coli OneShot® BL21 (DE3) Star™	Protein expression	Agilent Technologies

3. METHODS

3.1 Microbial cultivation and storage

3.1.1 Growth medium

Luria-Bertani (LB) liquid medium (1 L)

Materials

- 10 g Bacto® Trypton

- 10 g NaCl

- 5 g Bacto(R) Yeast extract

The ingredients were dissolved in 500 ml dH_2O and stirred until fully dissolved, followed by addition of dH_2O to a final volume of 1 L. Prior to use the LB medium was autoclaved for 15 minutes at 15 psi and cooled to room temperature.

3.1.2 Cultivation of *Escherichia coli*

The gram-negative bacterium *E. coli* is frequently used as a protein production organism in biotechnology. The bacterium grows well with a generation time of approximately 20 min. In this study recombinant *E. coli* was used to produce CBP21, an LPMO from *S. marcescens*. The general techniques for microbial cultivation are described below. All procedures described in section 3.1 were carried out using sterile techniques in a sterile environment (laminar flow hood), sterile equipment and solutions that had either been autoclaved or sterile filtered (0.45 µm pore size).

Materials

- LB medium (section 3.1.1)
- 50 mg/ml ampicillin
- Recombinant *E. coli* (glycerol stock)
- Ice
- Sterile toothpicks

Procedure

2 ml of LB medium was mixed with 5 µl ampicillin stock solution in a glasstube. A small part of frozen glycerol stock (kept on ice) was scraped using a sterile toothpick and added to the medium, followed by incubation overnight at 37^0C and 200 rpm.

3.1.3 Long-term storage of bacteria

For long time storage bacteria were stored at -80^{o}C. At this temperature the cells are in extreme conditions and can suffer from freezing damage due to ice crystal formation. For cell damage prevention, a cryoprotectant must be used, in this case glycerol.

Materials

- *E. coli* culture
- Sterile 85% glycerol
- Sterile screw cap cryo tubes (2 mL)

Procedure

300 µl of sterile glycerol (85%) was pipetted in a cryo tube and mixed with 700 µl of the *E. coli* culture (section 3.1.2). The cryo tube was stored at -80^{o}C until further use.

3.2 Protein expression and periplasmic extract

For expression of the CBP21 gene, *E. coli* BL 21 star™ containing a variant of the pRSET-B plasmid engineered for CBP21 production (Vaaje-Kolstad, Horn, et al., 2005) was cultivated.

CBP21 is directed to the periplasmic space and by using a cold osmotic shock procedure a periplasmic extract was prepared.

3.2.1 Protein expression and periplasmic extract from *E. coli*

For expression of CBP21, *E. coli* BL 21 star™ containing the pRSET-B-*cbp21* plasmid was cultivated overnight in LB medium (section 3.1.2. The gene encoding CBP21 contains a signal sequence that directs the protein to the periplasmic space where the signal peptide is removed by a signal peptidase. To harvest the mature protein (i.e. with the signal peptide removed) from the periplasm, cold osmotic shock was applied. This technique exposes the cell for sudden changes in the solute environment, which lyses the outer membrane of the cell, releasing the contents of the periplasm. The periplasmic content can be separated from the rest of the cell particles by centrifugation.

Materials

- 100 mg/ml ampicillin
- 300 ml LB medium
- 2 L culture flask
- Spheroplastbuffer:

    - 51.3 g Sucrose

    - 30 ml 1 M BisTris-HCl, pH 8.0

    - 300 µl 0.5 M EDTA, pH 8.0

    - 600 µl 50 mM PMSF in isopropanol

    - Dissolved in 300 ml dH2O

- Syringe, 10 ml
- 0.22 µm sterile filter
- 50 mM PMSF
- 20 mM MgCl
- Centrifuge rotor, JA-14

- Centrifuge cups, 250 ml
- Sterile plastic tubes (50 ml)

Procedure

A small piece of the glycerol stock (see section 3.1.3) was used to inoculate 300 ml LB medium in a 2 L culture flask that was premixed with 300µl ampicilin in sterile conditions, followed by incubation for 16 hours at 37°C and 200 rpm. The culture was transferred to a 250 ml centrifuge tube and centrifuged at 8000 rpm for 10 minutes at 4 ^{o}C. The supernatant was discarded and the pellet was resuspended in 30 ml ice cold spheroplastbuffer. The cell suspension was placed on ice for 5 minutes, followed by centrifugation for 10 minutes at 8000 rpm at 4^{o}C. The resulting supernatant was discarded and the pellet was resuspended in 25 ml cold dH_2O and placed on ice for 45 seconds. Next, the cell suspension was mixed with 1.25 ml 20 mM $MgCl_2$ before centrifugation at 8000 rpm for 10 minutes at 4^{o}C. Subsequently, the supernatant, which contains the periplasmic proteins, was sterile filtered through a 0.20 µm filter into a 50 ml sterile plastic tube. Finally, 2µl 50 mM PMSF was added per 1ml extract. The extract was stored at 4^{o}C until further use.

3.3 SDS-PAGE

Sodium dodecyl sulphate polyacrylamide gel electrophoresis (SDS-PAGE) is a widely applied technique to separate proteins based on their size. The native proteins are first denatured with an ionic detergent, such as sodium dodecyl sulphate (SDS) and a reducing agent (for reducing disulphide bridges). The proteins are at the same time provided with a global negative charge due to binding of SDS. An electric field is applied along an acrylamide gel and proteins with various sizes will travle through the gel towards the positively charged anode at rates depended on protein size. The proteins can be visualized by various staining techniques. The protein size can be estimated with a molecular marker containing proteins with known masses.

Materials

- 10 x BIO-RAD® TGS SDS running buffer (Invitrogen)
- Bench Mark™ Protein Ladder (Invitrogen)
- 10 x NuPAGE® reducing agent (Invitrogen)
- dH_2O
- Coomassie Brilliant Blue staining solution
- 4x Sample buffer NuPAGE® LDS sample buffer (Invitrogen)
- Power Pac 300 power supply
- BIO-RAD® mini protean® Tetra System
- Mini-PROTEAN® TGX Stain-Free ™ Precast gel any kD
- Stain free sample Trai (bio rad)
- Sample for analysis
- Gel Doc™ EZ Imager

Procedure

The samples were prepared by mixing 10 µl protein sample, 5 µl NuPAGE® LDS sample buffer (4 x), 2 µl NuPAGE® Reducing agent (10 x) and 3 µl H2O. After boiling the samples for 4 minutes, the samples (20 µl) were loaded into separate wells in the gel, together 5 µl with a protein standard containing proteins of known sizes (bench mark protein ladder). The precast gel was placed in the mini BIO-RAD® mini protean® Tetra System. The gel was run for 25 minutes at 255 V. To visualize the proteins the gel was taken out from the plastic container, next the gel was laid on the stain free trai and inserted in the Gel Doc™ EZ Imager wich was used to retrieve the image.

3.4 Affinity chromatography

Affinity chromatography is a method depending on the specific reversible interaction between the molecule to be purified and the solid phase (e.g. gel matrix), and is used for the separation of biomolecules. It is important that only the target molecule has affinity toward the solid phase, otherwise the resulting sample will be contaminated. The principle is based on that the sample is passed through a column packed with a solid phase. The target molecule will bind to the solid phase, and this may be promoted by optimizing conditions, for example the pH by using a buffer of choice. The proteins in the sample with no affinity for the column material pass through the solid phase and can be excluded. By changing environment factors such as the pH, ionic strength or a competing ligand, the target molecule will be released from the solid phase and elute. The eluted target molecule can be then collected in a 90% purified form. This process is monitored by an UV detector which detects the level of proteins passing through the system at all time. Affinity chromatography is a commonly used technique for purification of proteins. In this study chitin-affinity chromatography was used to purify CBP21.

3.4.1Chitin-affinity chromatography

The enzyme CBP21 binds efficiently to chitin. For purification of the enzyme chitin beads were used as the solid phase. The procedure was carried out using the BioLogic® LP chromatographic system, and was monitored using LP Data View.

Materials

- Econo-Column® (1.5 x 15 cm)
- Econo-Column® flow adaptor
- Chitin beads (New England Biolabs, NEB)
- 20% (v/v) ethanol
- 70% (v/v) ethanol

- Buffer A-1 M ammonium sulphate in 50 mM Tris-HCl pH 8.0 (binding buffer):
    - 132.14 g ammoniumsulphate
    - 2.4 g Tris-Base (
    - dH2O was added to a final volume of 1 L and the pH was adjusted with HCl
- Buffer B- 20 mM acetic acid pH 3.6 (elution buffer)
- 15 ml periplasmic extract
- Falcon tube, 50 ml

Procedure

The empty Econo-Column was prepared for the purification procedure by washing thoroughly with 70 % ethanol to remove contaminations. Next, approximately 15 ml chitin beads were applied to the column. A piston was inserted and locked at the top of the column material bed and the column was connected to the BioLogic chromatographic system. The system was then purged with 20% ethanol (flow rate 6.5 ml/min) and then equilibrated with binding buffer pH 8.0 (flow rate 2.5 ml/min) until the base line monitored by an UV reader was stable (approximately 10 min), after which the baseline signal was reset to zero. The periplasmic extract was adjusted to 1 M ammonium sulphate 50 mM Tris-HCL pH 8.0 prior loading it on the column for optimal binding purposes. After sample loading, buffer A was passed through the column (flow rate 2.5 ml/min) until the UV signal was stable at the base line level and remained so for about five minutes.

To elute the proteins bound to the chitin beads a change in the pH was introduced by changing to buffer B (acetic acid pH 3.6) (flow rate 2.5 ml/min). The eluted protein was collected in a 50 ml falcon tube, followed by up concentration and buffer axchange (section 3.5), then stored at 4^{o}C. Finally the system was purged (flow rate 6.5 ml/min) with 20% ethanol for about 15 minutes to clean the system and the column for remaining proteins. The chitin beads, now in 20% ethanol, were collected and stored at 4^{o}C for reuse.

3.6 Analysis of protein concentration

3.6.1 Bradford assay

The Quick Start™ Bradford Protein Assay (BioRad) is a spectroscopic analytical method applied for estimating the protein concentration in a solution. The assay is dependent on the binding interaction of Comassie Brilliant Blue G-250 dye to proteins. Upon dye binding to protein under acidic conditions the absorption maximum of the dye shifts from A_{max}=470nm to A_{max}= 595nm. The increase in absorption at 595 nm can be monitored using a spectrophotometer (Bradford, 1976). The increase in absorbance at 595 nm is proportional to amount of dye binding to proteins, which correlates to the concentration of the proteins in the solution.

Materials

- 5 x Bradford Dye Reagent (BioRad)
- Polystyrene cuvettes, 1 ml (Brandtech)
- Purified protein
- Sample buffer 20mM Tris-HCl pH 8.0
- Spectrophotometer, Biophotometer (Eppendorf)

Procedure

800 µl of a diluted protein solution was made by mixing 5 µl protein solution of unknown concentration with 795 µl sample buffer. Next, 200µl 5x dye reagent was added to the protein solution followed by mixing and incubation at room temperature for 5 minutes. Before measurements the photometer was zeroed using a blank containing 800 µl sample buffer and 200µl 5x Dye reagent. Absorbance (A_{595}) was measured by using the Bradford micro program on the spectrophotometer. The spectrophotometer was pre calibrated with a standard curve, which was used for calculating the concentrations in the samples, using the mean value from three samples.

3.6.2 Protein concentration analysis by measuring absorbance at 280 nm

Proteins in solution absorb UV-light with an absorbance maximum at 280 nm. The ability of a protein to absorb UV-light is due to the aromatic rings in the amino acids tryptophan, tyrosine and penylalanine and disulfide bonds (Pace, Vajdos, Fee, Grimsley, & Gray, 1995). The concentration of a pure protein in solution can be calculated based on absorption measured at 280 nm, given the extinction coefficient is known. The theoretical extinction coefficient for a protein can be calculated based on the content of UV absorbing amino acids in the sequence, e.g. using the web server Protparam (http://web.expasy.org/protparam/). For CBP21, the theoretical extinction coefficient was calculated to be 35200. By using the Beer-Lambert`s law (equation 1):

$$A = \varepsilon IC \qquad (1)$$

where Ɛ is the molar absorption coefficient, I is the pathlength (cm), and C is the protein concentration (M), it becomes possible to measure the protein concentrations.

Materials

- Disposable UVette® 220-1600 nm, 50-2000 µl (Eppendorf)
- Buffer: 20 mM Tris-HCl pH 8.0
- Purified protein

Procedure

The samples where centrifuged at maximum speed (4500 G) for 1 minute, for the purpose of sedimenting particles which could interfere with the measurement. Triplicates where prepared, and the spectrophotometer was reset to zero using buffer (20 mM Tris-HCl pH 8.0) prior to analysis. The mean value resulting from the triplicates was used for calculating the final concentration using the data provided from Protparam (i.e. a molecular extinction coefficient of 35200, which corresponds to the A_{280} of an 1mg/ml being 1.8730.

3. 7 Generation of apo-enzyme and holoenzyme

A cofactor is a non-protein chemical compound that is required for the protein's activity. Cofactors are often found in enzymes, and act as helper molecules in enzymatic reactions. A protein missing its cofactor is called and apoenzyme, whereas an enzyme containing the co-factor is called a holoenzyme. Two main groups of cofactors exist: organic cofactors and inorganic cofactors such as metal ions.

The copper metal ion of CBP21 can successfully be removed with a metal chelating compound, thus generating an apoenzyme. Removal of the copper inactivates CBP21, and activity can be restored by supplementing the cofactor, regenerating the CBP21 holoenzyme.

Materials

- 1 M EDTA, pH 8.0 in TraceSELECT® Ultra water
- 100 mM Cu(II)SO4
- TraceSELECT® Ultra water
- 20mM chelexed Pipes buffer pH 6.5 (5 g chelex/100 ml buffer)
    - 20 mM pipes buffer was prepared and further washed with 5g chelex for each 100 ml buffer, the buffer was then filtrated for removing particals prior to use.

- CBP21 stock solution (6,01 Mg/ml)
- Glass test tube (X ml)

Procedure

In order to remove the copper ion, the enzyme was incubated with EDTA at a concentration five times higher than the enzyme concentration, for 30 minutes, at room temperature. This incubation was done in a glass test tube prewashed with TraceSELECT® Ultra water for removal of contaminating metal ions. The total volume of the solution was 1 ml and the protein concentration was in 4-10 mg/ml range. Next, the solution was applied onto a PD MidTrap G-25 column for desalting (separation of the EDTA from the protein; see section 3.8).

Generation of the holoenzyme was done by saturating CBP21with $CuSO_4$. $CuSO_4$was added to the solution containing the apoenzyme at five times the concentration of the enzyme, followed by incubation at room temperature for 20 minutes. The excess of $CuSO_4$ was removed by desalting on PD columns (see section 3.8).

3.8 Enzyme desalting

PD MidTrap G-25 columns are suitable for rapid sample clean up of proteins and other large biomolecules. The columns can be applied for a wide range of applications such as buffer exchange, removable of low molecular weight compounds and desalting. The columns contain Sephadex G-25 medium which allows separation of high molecular weight molecules from low molecular weight substances. The chromatography technique is based on gel filtration and molecules are separated on the basis of differences in size. Two different protocols can be applied for elution of the protein, either using gravity or centrifugation. In this study the gravity protocol was used. This method was used to remove EDTA form the apo enzyme and for desalting the enzyme solution after copper saturation (see section 3.6).

Material

- 20mM Tris-HCL pH 8.0
- 10mM EDTA
- 20mM chelexed Pipes buffer pH 6.5 (5 g chelex/100 ml buffer)
- 1 ml enzyme (CBP21) concentrated solution
- PD MidTrap G-25 column

Procedure

The purpose of using this method was for both the removal of EDTA (when generating apoenzyme) and superfluous copper when generating holoenzyme. First the column was equilibrated with 3 times 5 ml of buffer (20mM chelexed pipes buffer pH 6.5 for apoenzymes; 20mM Tris-HCL pH 8.0 for cobber saturated enzyme) and finally equilibrated with 5 ml of buffer (20mM chelexed pipes buffer pH 6.5 for apoenzymes; 20mM Tris-HCL pH 8.0 for

cobber saturated enzyme). The equilibration step was followed by addition of 1 ml sample to the column. After the sample had fully entered the packed bed, 1.5 ml buffer was (20mM chelexed pipes buffer pH 6.5 for apoenzymes; 20mM Tris-HCL pH 8.0 for cobber saturated enzyme) added for eluting the enzyme. Fractions were continuously collected and analyzed for protein by A_{280}. The fraction containing the enzyme elutes in the segment between 1.0 ml and 2.5 ml.

3.9 Activity assays

Competitive experiments were conducted where the metal ions Zn^{2+}, Mn^{2+}, Co^{2+}, Ni^{2+} and Fe^{3+} obtained from the minerals $ZnSO_4$, $MnSO_4$, $CoSO_4$, $NiSo_4$ and $FeCl_3$, respectively, when dissolved in water, were analyzed for determination of their effect on $CBP21_{wt}$ activity. Effects on $CBP21_{wt}$ activity were analyzed non-quantitative (MALDI-TOF MS) and quantitative (HPLC). The respective metal ions are chosen because their known ability to function as cofactors in enzymes.

3.9.1 Sample preparation for MALDI-TOF MS inhibition assay

Reaction with different conditions (table 3.1) where prepared before MALDI-TOF MS analysis (section 3.10.1)

Table 3.1. MALDI-TOF MS assay condition. The reaction concentration for each metal ion (Zn^{2+}, Mn^{2+}, Co^{2+}, Ni^{2+} and Fe^{3+}) and their preincubbation time in buffer solution with $CBP21_{wt}$ (preincubation time tested- marked with x, samples not tested for marked with 0).

	Preincubation time of 1 µM CBP21 with added metal ions, in minutes					
[metal ion] (mM)	0	5	10	15	60	120
0.1	X	X	X	X	O	O
0.5	O	X	X	X	O	O
1.0	X	X	X	X	O	O
2.0	O	X	X	X	O	O
5.0	X	X	X	X	X	X
10	0	X	X	X	O	O

Materials

- $CBP21_{wt}$
- mg/mL β-chitin nanofibers in dH_2O (provided by J. Loose)
- 20 mM Tris-HCl, pH 8.0
- 100 mM ascorbic acid
- 100mM ($ZnSO_4$, $MnSO_4$, $CoSO_4$, $NiSo_4$ and $FeCl_3$) desolved in dH_2O

Procedure

Reactions (200µl) were mixed in 2.0 ml Eppendorf tubes contained the following end concentrations (components were added in given order) 1; 20 mM tris-HCl buffer pH 8.0, 2; one specific metal ion (concentrations and preincubation time according to table 3.1), 3; 1 µM CBP21, 4; 2 mg/ml β-chitin nanofibers and 5; 1 mM ascorbic acid. Next the reaction components were mixed and incubated for 90 minutes at 37°C with shaking at 750 rpm in an Eppendorf thermo mixer.

Reactions were stopped by centrifugation for 5 minutes at maximum speed (14000 rpm) to sediment the substrates. The supernatant was transferred to a fresh tube and stored at -20^{o}C until use.

For positive control one reaction free for metal ions was made. Two negative controls, one without enzyme and one with only β-chitin were also prepared. The control reactions had the same end concentrations as the reactions.

3.9.2 Sample preparation for UHPLC activity assay

Reactions containing of the respective metal ions at 5mM concentrations where prepared before UHPLC analysis of $CBP21_{wt}$ generated products (3.11.1)

Materials

- $CBP21_{WT}$ (saturated with copper)
- 10 mg/mL β-chitin nanofibers in dH_2O (provided by J. Loose)

- 20 mM Tris-HCl, pH 8.0 buffer
- 100 mM ascorbic acid
- 100 mM solutions of metal ions ($ZnSO_4$, $MnSO_4$, $CoSO_4$, $NiSo_4$ and $FeCl_3$
- Eppendorf tubes 2 ml (VWR)
- 96-well MultiScreenHTS filter plate with a 96-well collection plate (Millipore)
- High Output vacuum pump connected to a MultiScreenHTS Vacuum Manifold

Procedure

Reaction (500 µl total) were mixed in 2 ml Eppendorf tubes contained the following end concentrations (components were added in given order): 1; 20 mM tris-HCl pH 8.0, 2; 5 mM of one specific metal ion, 3; 1 µl CBP21, 4; 15 minutes preincubation time, 5; 2 mg/ml β-chitin nanofibers and 6; 1 mM ascorbic acid.After addition of substrate, the samples where incubated at 37°C with shaking at 750 rpm. At 30 min time intervals ranging from 30 min to 150 minutes, 60 µl of the reaction was sampled and filtrated using a 96-well filter plate and a vacuum pump. Next 50 µl of the filtrated sample were transferred to 2 ml Eppendorf tubes and stored at -20^{o}C until use.

3.9.3 Sample preparation for HPLC synergy assay

Materials

- H_2SO_4, 50 mM and 5 mM solutions
- $CBP21_{WT}$ (saturated with copper)
- Purified ChiC from *S. marcescens* (supplied by S. Mekasha)
- 10 mg/mL β-chitin nanofibers in dH_2O (provided by J. Loose)
- 20 mM Tris-HCl, pH 8.0
- 100 mM ascorbic acid
- 100 mM metal ion solutions ($ZnSO_4$, $MnSO_4$, $CoSO_4$, $NiSo_4$ and $FeCl_3$)
- dH_2O
- Eppendorf tubes, 2.0 ml (VWR)
- HPLC tubes (VWR)
- Snap ring cap for HPLC tubes, 11 mm (VWR)
- 96-well MultiScreenHTS filter plate with a 96-well collection plate (Millipore)

- High Output vacuum pump connected to a MultiScreenHTS Vacuum Manifold

Procedure

Reaction (500 µl total) were mixed in 2 ml Eppendorf tubes contained the following end concentrations (components were added in given order): 1; 20 mM tris-HCl pH 8.0, 2; 5 mM of one specific metal ion, 3; 1 µl CBP21, 4; 120 minutes preincubation time, 5; 0.1 µM ChiC 6; 2 mg/ml β-chitin nanofibers and 7; 1 mM ascorbic acid.

After adding the substrate, samples where incubated at 37°C with shaking at 750 rpm. At 30 minutes intervals from 30 until 150 minutes, 50 µl was sampled and mixed with 50 µl 50 mM H_2SO_4 in 2 ml Eppendorf tubes to stop the enzymatic reaction. Next the sample was filtrated by by 96-well filter assisted by a vacuum pump, followed by centrifuging for 5 min at (14000 rpm), before 80µl of the sample were transferred to HPLC vials and stored at -20^{o}C until further use.

3.10 MALDI-TOF MS

MALDI-TOF is a sensitive non-quantitative mass spectrometric method for molecular weight analysis of biomolecules such as DNA, proteins, peptides and oligosaccharides. The method implies that the crystallized analytes is irradiated with short pulses using an UV-laser. The anlytes are then ionized and desorbs into gas phase in vacuum. From the gas phase the charged molecules are accelerated by a magnetic field in towards a time of flight (TOF) detector, which measures the time it takes for the molecule to travel the fixed distance. The analytes have different travel times according to their mass over charge ratio (m/z), and are separated based on their flight time.

3.10.1 MALDI-TOF MS analysis of enzyme activity

The inhibitory effect from the respective metal ions on $CBP21_{wt}$ activity, in solution with β-chitin, was non-quantitatively analyzed using MALDI-TOF MS. The different reaction conditions are showed in table 3.1

Materials

- DHB-matrix solution:

  -4.5 mg DHB (2.5-Dihydroxybenzoic acid)

  -150 µl acetonitrile

  -350 µl dH_2O

  -The solution was vortexed until the DHB was fully dissolved

- Reactions from section 3.9.1
- MTP 384 target plate ground steel TF (Bruker Daltonics)
- MALDI-TOF MS Ultraflex system (Bruker Daltonics)

Procedure

2 µl of DHB-matrix and 1 µl of from the reactions prepared from section 3.9.1 were mixed on a target plate. Subsequently, the drop was dried with a warm flow of air (in this case from a hair drier). Then the MALDI plate was inserted in the MALDI-TOF MS analyzer. The samples were shot 299 times using a nitrogen 377 nm laser beam with intensity varying from 20-30%. FlexControl software was used for managing the system and FlexAnalysis for analysis and processing of the data.

3.11 Ultra high-performance liquid chromatography (UHPLC)

UHPLC is a chromatographic technique applied for the separation of analytes that are dissolved in a solution. The technique has multiple purposes such as identifying, quantifying

and purifying analytes. The method relies on the constant, pulse free and high pressure flow rate delivered to the system from multi-piston pumps, that drive the mobile phase trough the stationary phase (i.e. the contents of the column) and further to the detector. The ability to operate under high pressure allows the use of high density columns, which results in better chromatographic separation and high resolution. The time from injection of the sample to the detection of a compound is called the retention time. The analytes in the applied sample will differ in their retention time on the basis of their interactions with the stationary phase and the mobile phase.

3.11.1 Analysis of $CBP21_{wt}$ generated products by UHPLC

Materials

- Reactions from (section 3.9.2)
- Standard: C1 oxidized fully acetlated chitooligosaccharides with a degree of polymerization (DP) ranging from 4 to 8 (provided by J. Loose)
- 99.8 % (w/v) acetonitrile (HPLC grade)
- 15 mM Tris-HCl, pH 8.0 (vacuum filtrated using a Stericup-GP PES Filter Unit (Millipore) with 0.22 µm pore size)
- 96-well MultiScreenHTS filter plate with a 96-well collection plate (Millipore)
- High Output vacuum pump connected to a MultiScreenHTS Vacuum Manifold
- Agilent 1290 Infinity LC system (GE Healthcare)
- Column: HILIC, Acquity UPLC® BEH Amide 1.7 µm, 150 x 2.1mm (Waters)
- Pre column: BEH Amide VanGuard, 1.7 µm, 5 x 2.1 mm
- HPLC tubes (VWR)
- Snap ring cap for HPLC tubes, 11 mm (VWR)

Procedure

26 µl from the samples made in section 3.9.2 were transferred to 2 ml Eppendorf tubes which were prefilled with 74µl acetonitrile. This step was followed by centrifuging for 5 min at max

speed (14000 rpm) to sediment all unsoluble particles, then minimum 80µl were pipetted over to HPLC-vials for analysis. Standard of C1 oxidized fully acetlated chitooligosaccharides with a degree of polymerization (DP) ranging from 4 to 8 were also prepared and diluted to a final concentration of 100 µM and used as standards for detecting oxidized products.

Separation of the products was obtained using a Agilent 1290 Infinity UHPLC-system set up with a Waters Acquity UPLC BEH amide column and a BEH Amide pre-column. The sample volume applied on the column was set to 5 µl. The flow rate used was 0.4 ml/min throughout the run and the column temperature was set to 30°C. Separation of the analytes was accomplished by using a gradient program starting with 74 % acetonitrille and 26% 15 mM Tris-HCl pH 8.0 for 5 minutes, followed by a 5 minutes gradient to 62 % acetonnitrille, 38% 15 mM Tris-HCl pH 8.0. Finally the column was reconditioned with 74% acetonnitrile and 26% 15 mM Tris-HCl pH 8.0 for five minutes. Eluted products were detected by measuring absorption at 205 nm.

3.11.2 Analysis of chitin degradation in synergy experiments

For analysis of disaccharide products obtained upon β-chitin degradation by $CBP21_{wt}$ in synergi with ChiC in the presence of 5 mM metal ions, a HPLC method based on ion exclusion was used.

Materials

- Reactions from - Sample preparation for HPLC synergy assay, section (3.9.3)
- H_2SO_4, 50 mM and 5 mM solutions
- Standards: GlcNAcs with DP 2 and 3
- HPLC tubes (VWR)
- Snap ring cap for HPLC tubes, 11 mm (VWR)
- 96-well MultiScreenHTS filter plate with a 96-well collection plate (Millipore)
- High Output vacuum pump connected to a MultiScreenHTS Vacuum Manifold
- Rezex RFQ_Fast fruit H+ (8%), 100 x 7.8 mm column
- Phenomene Dionex Ultimate 3000 RSLC HPLC

Procedure

The prepared reactions in HPLC tubes from section 3.9.3 where used in this analysis. To analyse degradation of chitin to mono- and disaccharides, $(GlcNAc)_{1-2}$, a Dionex Ultimate 3000 RSLC HPLC system equipped with a Rezex RFQ Fast Fruit column was used. Chormeleon version 7.1.1.1127 was used to monitor, record and analyze the data. Prior to use, the column was heated up to 85°C while 5 mM H_2SO_4 was run through the system at a flow rate of 0.3 ml/min. When the temperature reached 85°C, the flow rate was adjusted to 1.0 ml/min, which was the rate throughout the subsequent runs. From each sample and standard 5µl was applied on the column and separation was achieved using a 12 minutes elution and re-equilibration program. Eluted products were detected by measuring absorption at 195 nm. GlcNAcs with DP ranging from 1 to 2 diluted to the final concentration of 100 µM were used as standards.

4. RESULTS

4.1 Protein production and purification

Cultivation of cells producing CBP21 was carried out according to section 3.1 and the periplasmic content of these cells was extracted according to section 3.2. SDS-PAGE analysis (Figure 4.2). of the periplasmic extract showed a substantial amount of CBP21 present in the sample. Purification of CBP21 was achieved by chitin-affinity chromatographic as described in section 3.8.1. Figure 4.1 shows a typical chromatogram; the first peak represents the unbound protein ("flow through" fraction), whereas the second peak, eluting at 50 minutes, represents bound proteins that are released from the column material by a pH adjustment (20 mM acetic acid pH 3.6). CBP21 solutions obtained in this manner were concentrated, typically to 6.0 g/L using ultrafiltration with Amicon® Ultra centrifugal filter devices (section 3.2.3). Followed by either generation of apo-enzyme (section 3.7) or saturation with cobber following desalting (section 3.8).

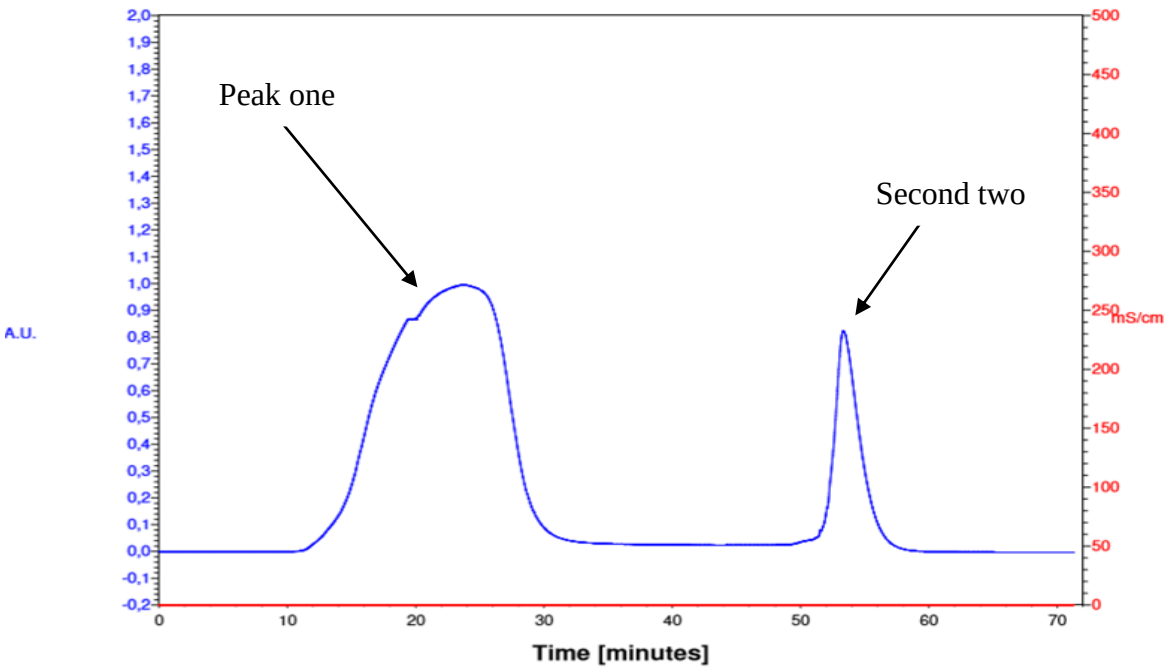

Figure 4.1. Chromatogram from the purification of CBP21 by chitin-affinity chromatography. CBP21 was purified from approximate 15 ml of periplasmic extract which was applied on a column packed with 15 ml of chitin beads (flow rate 2.5). The procedure was as described in section 3.8.1. The left Y-axis shows absorbation units whereas the right Y-axis shows conductivity meshured in milli-simens/centimeter. The flow through-and the bound protein-fractions are indicated by arrows. See text for more details

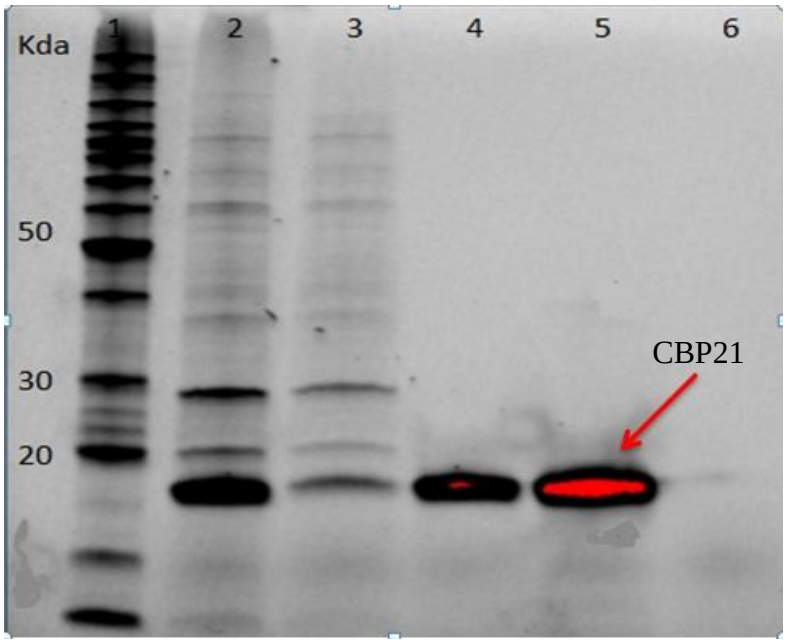

Figure 4.2. SDS-PAGE gel analysis of different fractions collected during purification of CBP21. Lane 1, Bench Mark™ Protein Ladder (Invitrogen) used as a protein marker and are labeled by molecular weight (kDa) ; Lane 2, periplasmic extract; Lane 3, flow through during chitin affinity chromatography; 4, purified protein, before ultrafiltration Lane 5; concentrated protein;lane; Lane 6, waste fraction from the ultrafiltration step. CBP21 has a molecular weight of 18.8 kDa and is indicated by an arrow. The red coloring represents pixel saturation indicating a very high protein concentration. The kDa values represent the bech mark ladder which indicates the given size of the proteins.

Protein purification procedure was monitored by SDS-PAGE analysis (Figure 4.1). The analysis of the periplasmic extract shows a wide range of proteins ranging from 10-100 kDa representing the *E. coli* periplasmic proteins and CBP21 (Figure 4.1 lane nr 2). The same analysis of the flow through (Figure 4.1, lane 3), showed that there is still some CBP21 that has not bound to the column material. The samples containing eluted protein before and after concentration (Figure 4.1, lane 4 and 5) show only one band appearing just below 20 kDa, which represents purified CBP21. Lane six in the SDS-PAGE analysis represents the waste fraction from the ultrafiltration step and shows no proteins.

4.2 Activity assay

4.2.1 Enzyme activity detection by MALDI-TOF MS

Reactions with copper saturated CBP21 ($CBP21_{wt}$) and different metal ions where prepared and analyzed by MALTI-TOF MS. A variety of metals were incubated with $CBP21_{wt}$ (one type of metal ion in each reaction) at concentrations ranging between 0.1mM to 10 mM (see Table 3.1 for experimental setup; for clarity this Table also appears below, as Table 4.1) in order to investigate inhibitory effects. A second parameter included was the time $CBP21_{wt}$ was incubated with the metal ion before the reaction was started by adding β-chitin and ascorbic acid (referred to as pre-incubation). MALDI-TOF MS was used for qualitative analysis of oxidized chitooligosaccharides ($DP4_{ox}$-$DP8_{ox}$) according to section 3.10.1. A typical product profile generated by copper-saturated CBP21 is shown in Figure 4.3. The presence or absence of the diagnostic products shown in Figure 4.3, was used to categorize $CBP21_{wt}$ as active or inactive in the metal ion inhibition assay.

Table 4.1. MALDI-TOF MS assay condition. Shows the reaction concentration for each metal ion (Zn^{2+}, Mn^{2+}, Co^{2+}, Ni^{2+} and Fe^{3+}) and their preincubbation time in buffer solution with CBP21 (preincubation time tested- marked with x, samples not tested for marked with 0).

	Preincubation time of 1 µM $CBP21_{wt}$ with added metal ion, in minutes					
[metal ion] (mM)	0	5	10	15	60	120
0.1	X	X	X	X	O	O
0.5	O	X	X	X	O	O
1.0	X	X	X	X	O	O
2.0	O	X	X	X	O	O
5.0	X	X	X	X	X	X
10	0	X	X	X	O	O

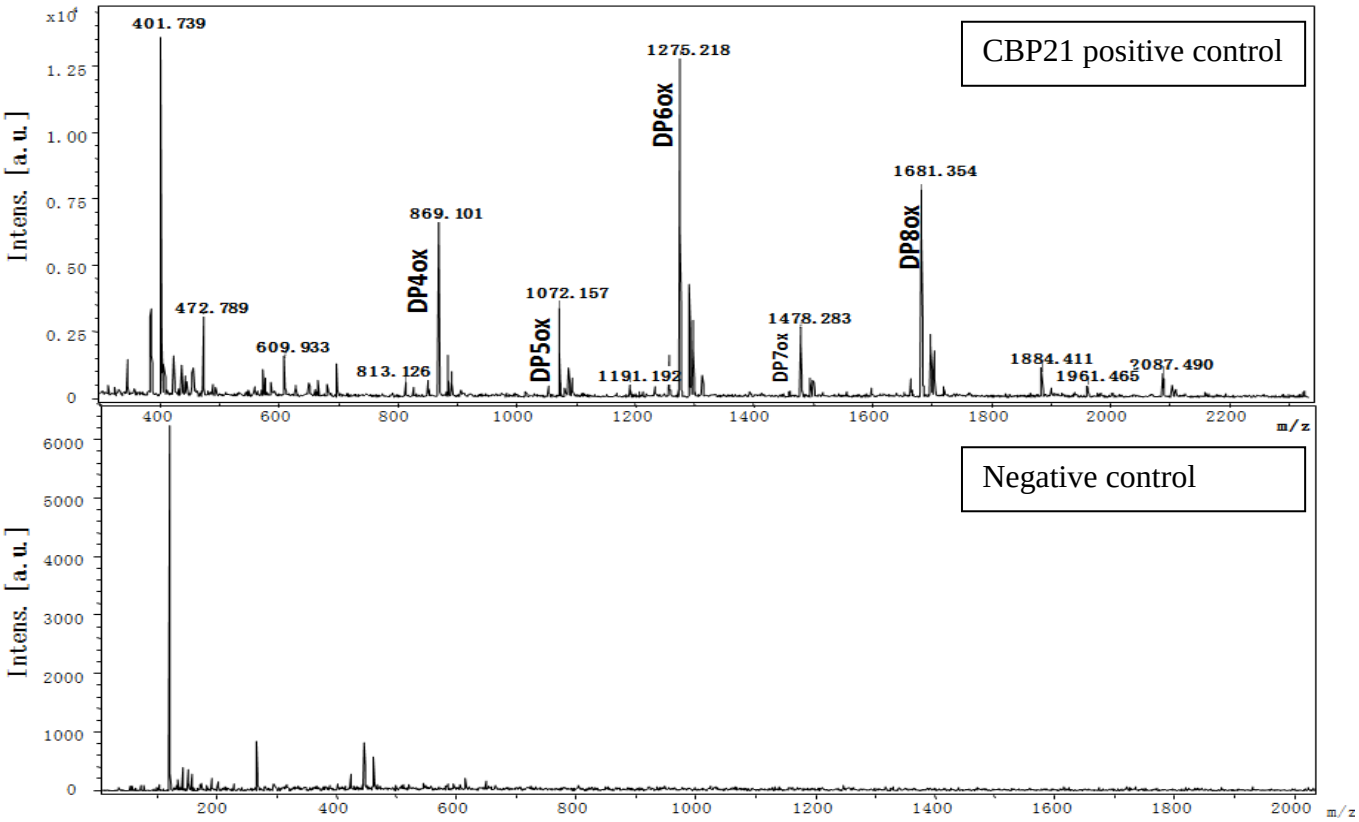

Figure 4.3. MALDI-TOF MS spectrum representing products generated by $CBP21_{WT}$ when acting on β-chitin. The topp spectrum shows oxidized chitooligosaccharides detected when 2 mg/ml β-chitin was incubated with 1 µM $CBP21_{WT}$ and 1 mM ascorbic acid in 20 mM Bis-Tris pH 8.0 for 120 minutes at 37°C and 750 rpm. The bottom spectrum demonstrate that no oxidized soluble chitooligosaccharides were detected under uniform conditions, but without $CBP21_{WT}$. The peaks are labelled with their atomic masses and annotated with their degree of polymerization. Some examples: *m/z* 1072.1 [DP5ox + Na]+; *m/z* 1275.2, [DP6ox + Na]+; *m/z* 1681.3, $[DP8ox + Na]^+$.

The results from the MALDI-TOF analysis showed that CBP21 *was active in the*

Analysis of the MALDI-TOF data (Table 4.2) indicates that $CBP21_{wt}$ was active in the presence of all metal ions at concentrations below 2mM, independent of pre-incubation time (results is not showed). For metal ion concentrations at 2mM and 5mM all samples except reactions containing Fe^{3+} showed activity regardless of pre-incubation time. At 10 mM metal ion concentration, Co^{2+} inhibited CBP21 activity at all preincubation times, whereas samples containing 10mM Zn^{2+} ions only inhibited CBP21 when the preincubation time was 15 min In table 4.2 the criteria for deciding if there was any activity in the different reactions, was dependent on if there were observable peaks representing oxidized chitooligosaccharides. Especially the presence of oxidized DP6 peak was of interest when analyzing for enzyme activity.

Table 4.2. Show activity of $CBP21_{wt}$ towards β-chitin under different reaction conditions. The preincubation time indicates the time the respective metal ions have been incubated together with the enzyme in buffer solution before addition of 1.0 mM ascorbic acid and 2.0 mg/ml substrate, see section 3.9 for details. Activity was analyzed by MALDI-TOF MS detection of oxidized chitooligosaccharides. In the table "+" indicates detected oxidized chitooligosaccharides, whereas"-" indicates no detection of oxidized chitooligosaccharides, in the respective reactions. Reaction conditions which were used for further analysis by HPLC methods are marked in blue.

Preincubation 5 min					
	Zn^{2+}	Mn^{2+}	Co^{2+}	Ni^{2+}	Fe^{3+}
2mM	+	+	+	+	-
5mM	+	+	+	+	-
10mM	+	+	-	+	-
Preincubation 10 min					
	Zn^{2+}	Mn^{2+}	Co^{2+}	Ni^{2+}	Fe^{3+}
2mM	+	+	+	+	-
5mM	+	+	+	+	-
10mM	+	+	-	+	-
Preincubation 15 min					
	Zn^{2+}	Mn^{2+}	Co^{2+}	Ni^{2+}	Fe^{3+}
2mM	+	+	+	+	-
5mM	+	+	+	+	-
10mM	-	+	-	+	-
Preincubation 30 min					
	Zn^{2+}	Mn^{2+}	Co^{2+}	Ni^{2+}	Fe^{3+}
5mM	+	+	+	+	-
Preincubation 60 min					
	Zn^{2+}	Mn^{2+}	Co^{2+}	Ni^{2+}	Fe^{3+}
5mM	+	+	+	+	-
Preincubation 120 min					
	Zn^{2+}	Mn^{2+}	Co^{2+}	Ni^{2+}	Fe^{3+}
5mM	+	+	+	+	-

Typical MALDI-TOF MS specter for reactions with the five different metal ions (at 5 mM concentration, and 15 minutes pre-incubation) are shown in Figure 4.4. The cluster at 1275 m/z represents $DP6_{ox}$ and 1681/1712- m/z represent $DP8_{ox}$.

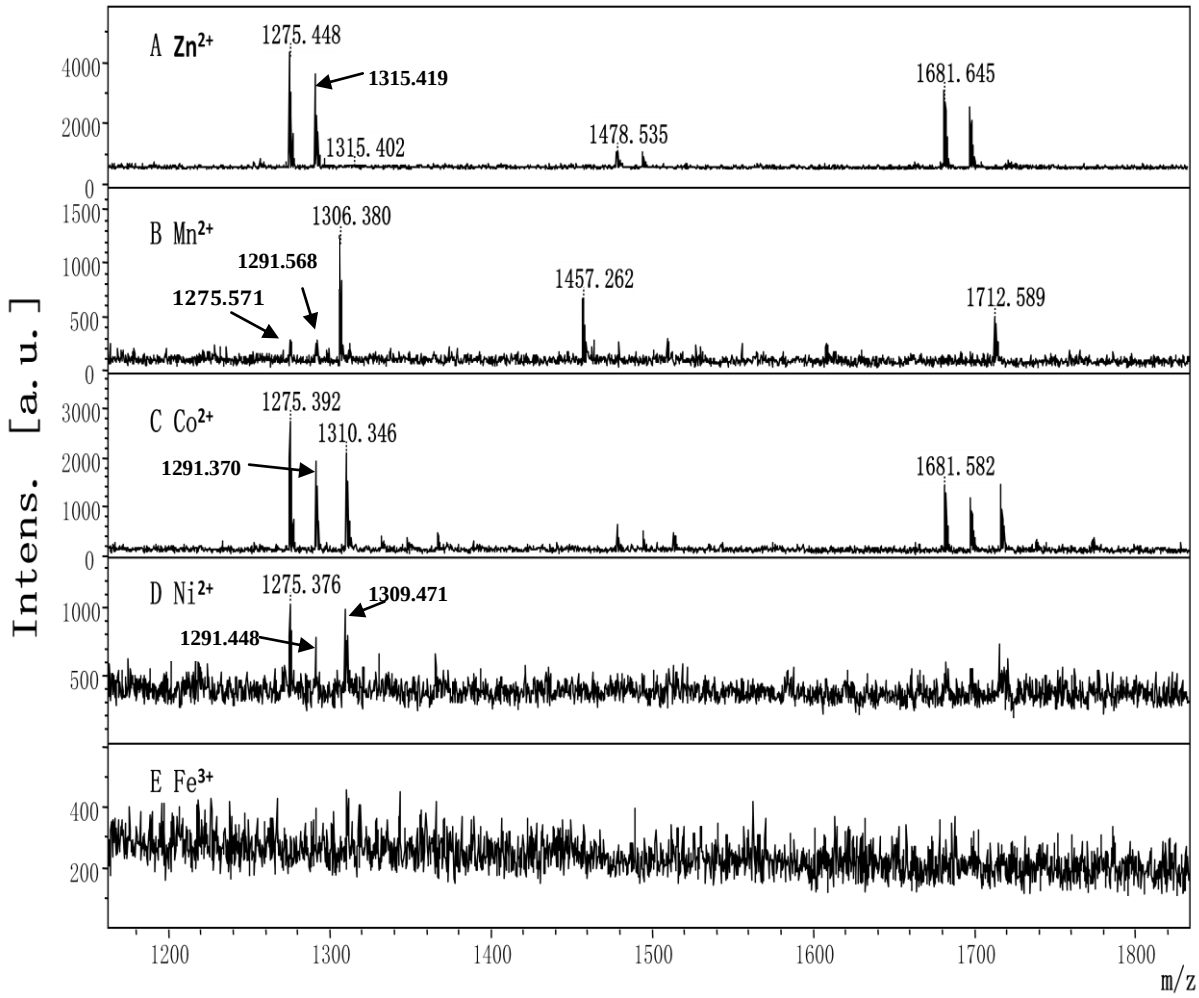

Figure 4.4 MALDI-TOF MS spectra showing products generated by copper-saturated CBP21 in the presence of 5mM Zn^{2+}, Mn^{2+}, Co^{2+}, Ni^{2+} and Fe^{3+}. Each of the different metal ions were pre incubated for 15 minutes with 1µM CBP21 in 20mM Tris-HCl pH8 buffer, before addition of 2mg/ml β-chitin (sonicated) and 1mM ascorbic acid. The figure shows the MALDI-TOF MS spectre from 1000 m/z to 2000 m/z. CBP21 activity is specially apparent from the 1275 *m/z* peak representing $[DP6ox + Na]^+$. Spectrum A represents activity in the presence of Zn^{2+}, Spectrum B represents activity in presence of Mn^{2+}, spectrum C represents activity in presence of Co^{2+}; spectrum D represents activity in presence of Ni^{2+} ; spectrum 5 represents activity in presence of Fe^{3+}. The peaks are labeled by their m/z values. No products were observed for the reaction containing $Fe^{3+.}$

Interestingly, a more detailed analysis of the spectrums at the $DP6_{ox}$ cluster revealed the presence of adducts containing the divalent metal ion which was added in the reaction. This (Fig 4.5). Table 4.3 shows m/z values for adducts which does not corresponding to m/z 1275 ($[DP6ox + Na]^+$) or m/z 1291($[DP6ox + K]^+$).

Table 4.3. Analysis of DP6ox adducts. The experimentally observed masses are shown in the column named "$[M+Metal^{2+}]$". The mass difference between $[DP6ox + Na]^+$ (m/z = 1275; present in all samples) and the observed unknown peak - $[M+Metal^{2+}]$ (assumed to be adducts with ions which is added) is represented in the column named Δ([M+Metal2+]-[M+Na]). The theoretical mass difference (minus one; since one protone is lost) between Na and the respective metal ions is noted in the last column.

Metal $^{2+}$	$[M+Metal^{2+}]$	$\Delta([M+Metal^{2+}]-[M+Na])$	Δ ((ion - Na)-1)
Zn^{2+}	1315.45	39.95	41.40
Mn^{2+}	1306.57	30.97	30.95
Co^{2+}	1310.39	34.95	34.94
Ni^{2+}	1309.42	33.94	33.70

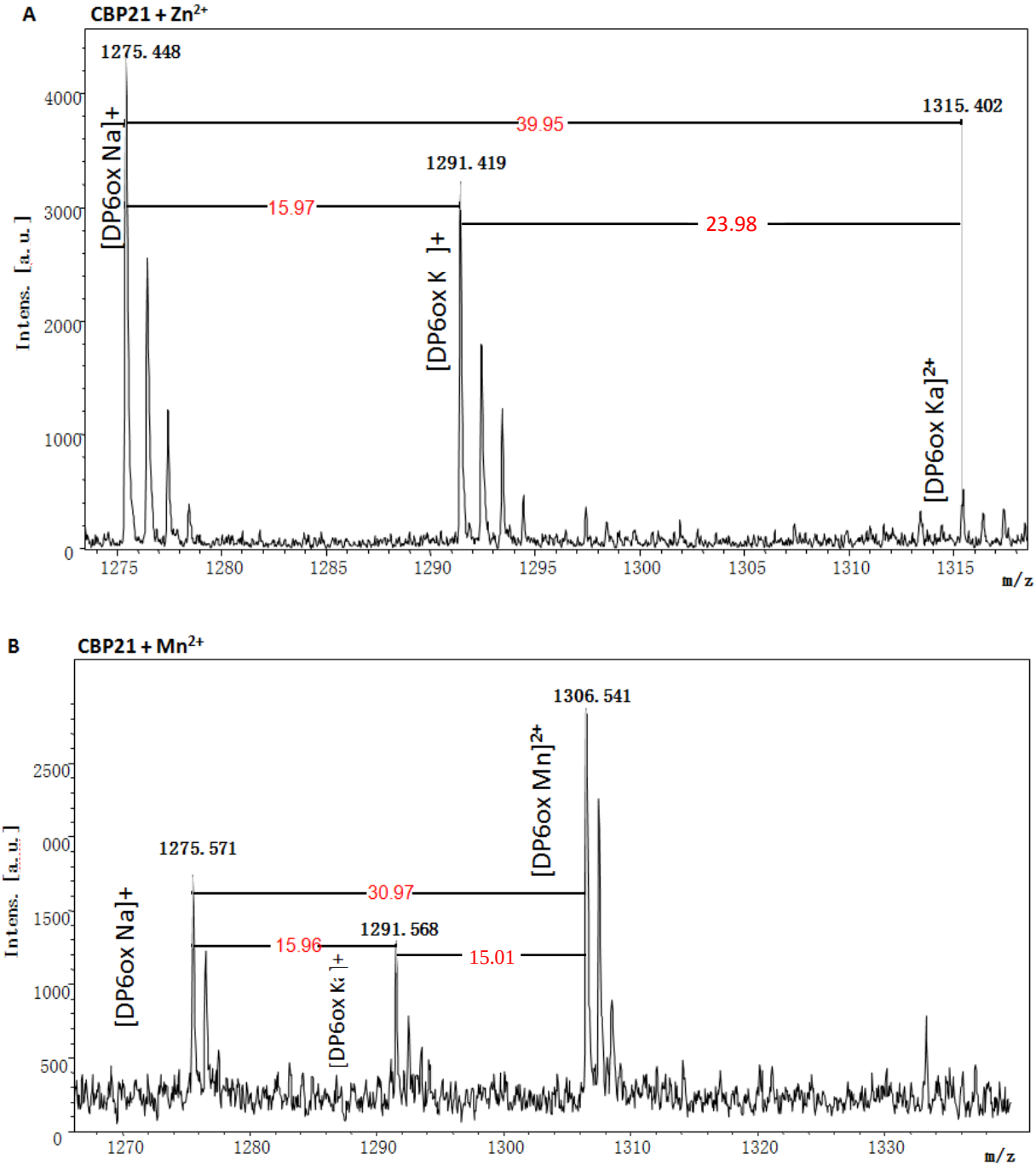
A
CBP21 + Zn2+
1275. 448
[DP6ox Na]+
39.95
1315. 402
1291. 419
15.97
23.98
[DP6ox K]+
[DP6ox Ka]2+
Intens. [a. u.]
m/z
B
CBP21 + Mn2+
1306. 541
[DP6ox Mn]2+
1275. 571
30.97
[DP6ox Na]+
15.96
1291. 568
15.01
[DP6ox Ki]+
Intens. [a. u.]
m/z

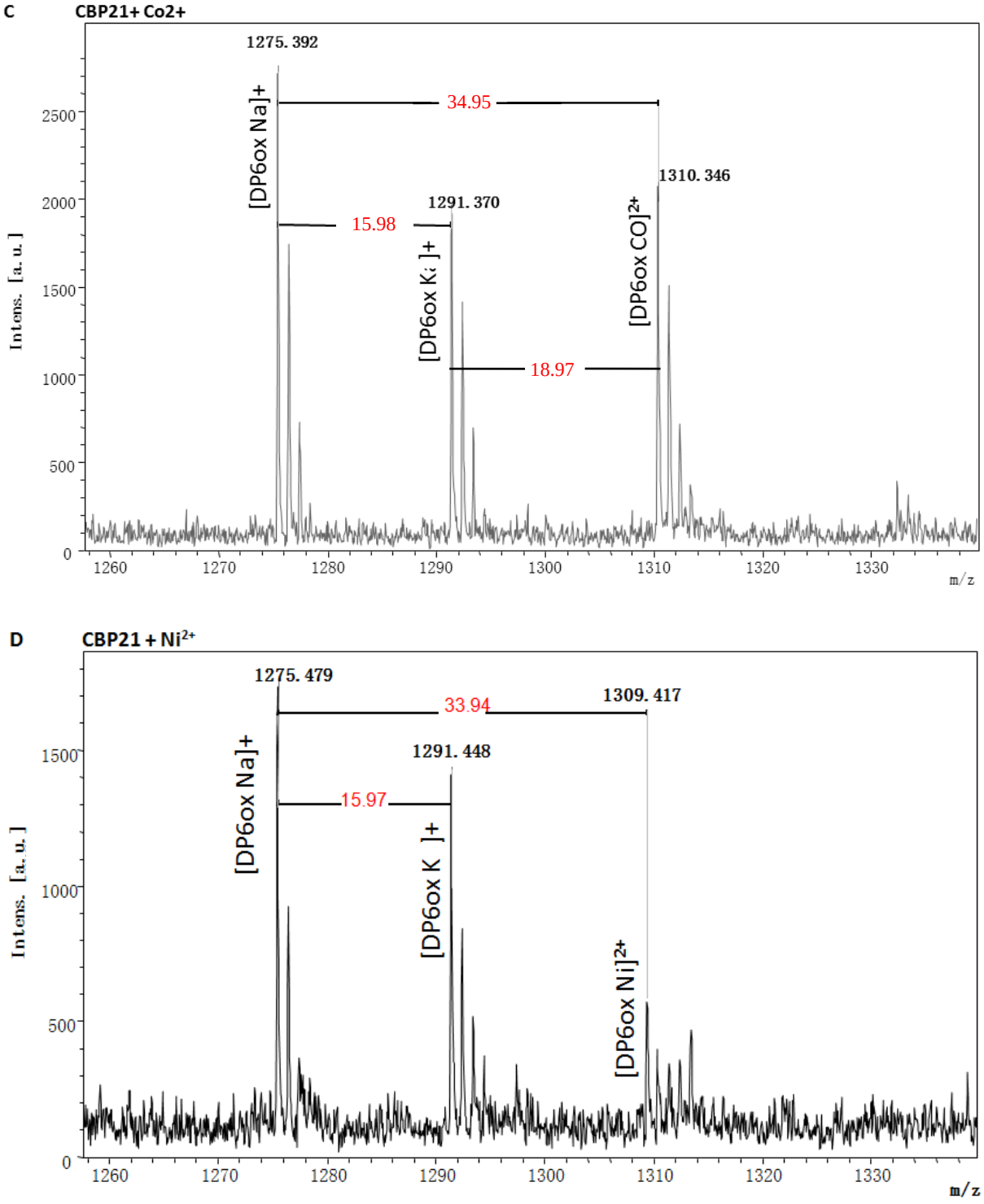

Figure 4.5 MALDI-TOF MS spectra of the Dp6ox cluster. Figures represent a closer analysis of the oxidized hexameric products generated in reactions with different metal ions (5mM). The metal ions at 5mM consentration have been preincubated for 30 minutes with 1µM $CBP21_{wt}$ in 20mM Tris-HCl pH8 buffer, before addition of 2mg/ml β-chitin (zonicated) and 1mM ascorbic acid, following incubation at 37°C with shaking at 750 rpm for 90 minutes. Adducts of the different hexameric products are labeled with their m/z values and annotated with their predicted composition, the difference in m/z between products is also showed. A, reaction with Zn^{2+} ions; B, reaction with Mn^{2+} ions; C, reaction with Co^{2+} ions; D, reaction with Ni^{2}+

Quantitative determination of oxidized products generated by $CBP21_{wt}$ in the presence of added metal ions was conducted by hydrophilic interaction chromatography (HILIC) using an UHPLC system. Oxidized products ranging in DP from 4-8 were detected after degradation of β-chitin by $CBP21_{wt}$ in reactions with 5 mM metal ions and 15 minutes preincubation time. A typical chromatogram is shown in figure 4.6.

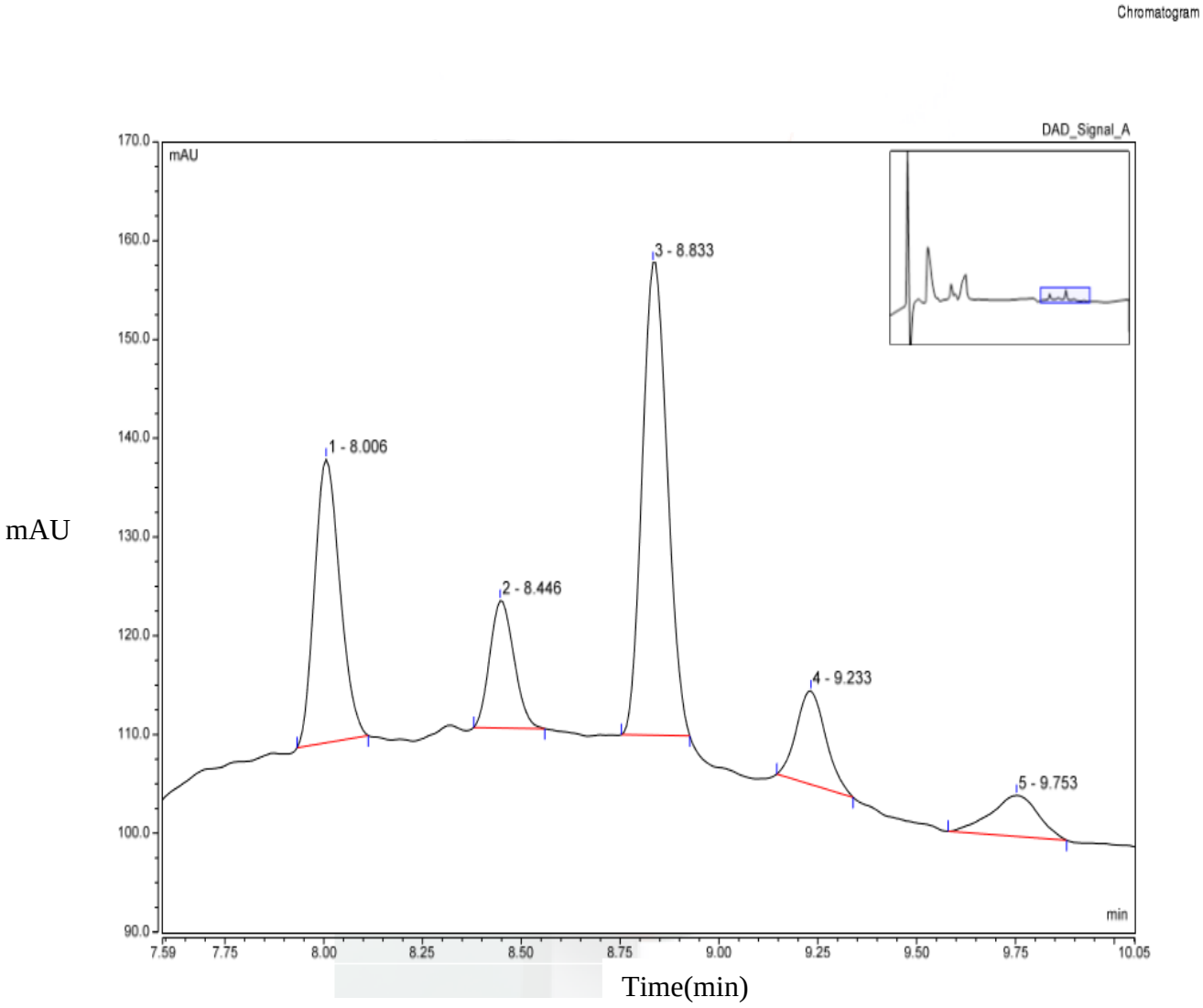

Figure 4.6. Chromatogram of $CBP21_{wt}$-generated oxidized products between DP4 to DP8. The products are generated after treating 2mg/ml β-chitin with 1µM $CBP21_{wt}$ and 1mM ascorbic acid in 20 mM Tris-HCl buffer pH8 for 60 minutes at 37^0C and 750 rpm. The amounts of products were expressed as peak areas in mAU (milli absorbance units (y-axis). DP for each peak is annotated and the red lines are manually inserted base lines before integration.

In order to investigate the influence of the metals ions on $CBP21_{wt}$ activity, time course assays were run for each metal ion, using $CBP21_{wt}$ in the absence of metal ions as a positive

control. The activity of $CBP21_{wt}$ in rections containing the different metal ions was relatively compared to the positive control (table 4.4).

Table 4.4. $CBP21_{wt}$ activity in reactions containing the respective metal ions relatively compared to the positive control. Reaction mixtures contained 1µM CBP21, 2 mg/ml β-chitin, 1mM ascorbic acid in 20mM Tris-HCL buffer pH 8.0 and 5mM metal ions. $CBP2_{wt}$ and the respective metal ion were preincubatet for 15 minutes in buffer solution before addition of β-chitin and ascorbic acid, next they were incubated at 37^0C with shaking at 750 rpm. Triplicates samples were taken at 20, 40 and 60 minutes and analyzed with UHPLC (see section 3.11.1) Red numbers indicate higher enzyme activate at given time point and for which DP_{ox}, compared to the $CBP21_{wt}$.

Activity relatively compared to $CBP21_{wt}$ at 20 minutes					
Reactions	DP4ox	DP5ox	DP6ox	DP7ox	DP8ox
CBP21wt+Zn^{2+}	0,75	0,63	0,79	0,58	0,55
CBP21wt+Mn^{2+}	2,43	2,20	2,20	1,92	1,20
CBP21wt+Co^{2+}	1,21	1,48	1,28	1,11	0,67
CBP21wt+Ni^{2+}	1,21	1,90	2,02	1,58	0,78
CBP21wt+Fe^{3+}	0	0	0	0	0
Activity relatively compared to $CBP21_{wt}$ at 40 minutes					
Reactions	DP4ox	DP5ox	DP6ox	DP7ox	DP8ox
CBP21wt+Zn^{2+}	0,85	0,74	0,81	0,71	0,43
CBP21wt+Mn^{2+}	1,91	1,73	1,67	1,86	0,63
CBP21wt+Co^{2+}	0,84	0,73	0,79	0,73	0,18
CBP21wt+Ni^{2+}	1,74	1,29	1,51	1,33	0,39
CBP21wt+Fe^{3+}	0	0	0	0	0
Activity relatively compared to $CBP21_{wt}$ at 60 minutes					
Reactions	DP4ox	DP5ox	DP6ox	DP7ox	DP8ox
CBP21wt+Zn^{2+}	0,79	0,79	0,82	0,58	0,64
CBP21wt+Mn^{2+}	1,14	0,97	1,01	0,76	0,38
CBP21wt+Co^{2+}	0,52	0,48	0,42	0,33	0,21
CBP21wt+Ni^{2+}	1,13	0,89	1,01	0,63	0,38
CBP21wt+Fe^{3+}	0	0	0	0	0

Data from the relative comparison of enzyme activity (table 4.4) show reduced activity for reactions with Zn^{2+} all over, further in the initial phase (min<20) in reaction containing Mn^{2+}, Ni^{2+} and Co^{2+} increase activity is observed, specially for products with DP_{ox} between 4 to 7. The increased activity in this three reactions are declining with time, for Mn^{2+} and Ni^{2+} the activity is comparable to the control at 60 minutes, whereas for Co^{2+} the activity is under well under 50% at 60 minutes, compared to the control. Reactions with Fe^{3+} show full inhibition.

Results from analysis by UHPLC of oxidized products generated (Figure 4.7 A-E) show some features that are common for all reactions. First of all, the initial phase of the reaction (0-20 minutes) seems to be fast. After 20 minutes, product formation seems to slow down. Secondly, in all reactions $DP6_{ox}$ is the dominant product

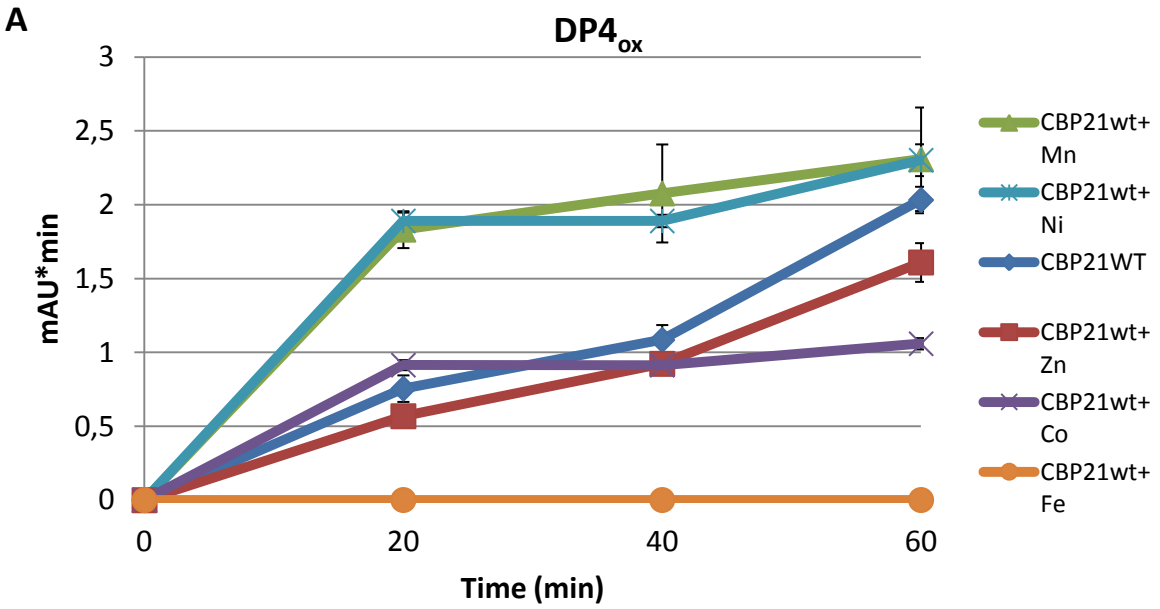

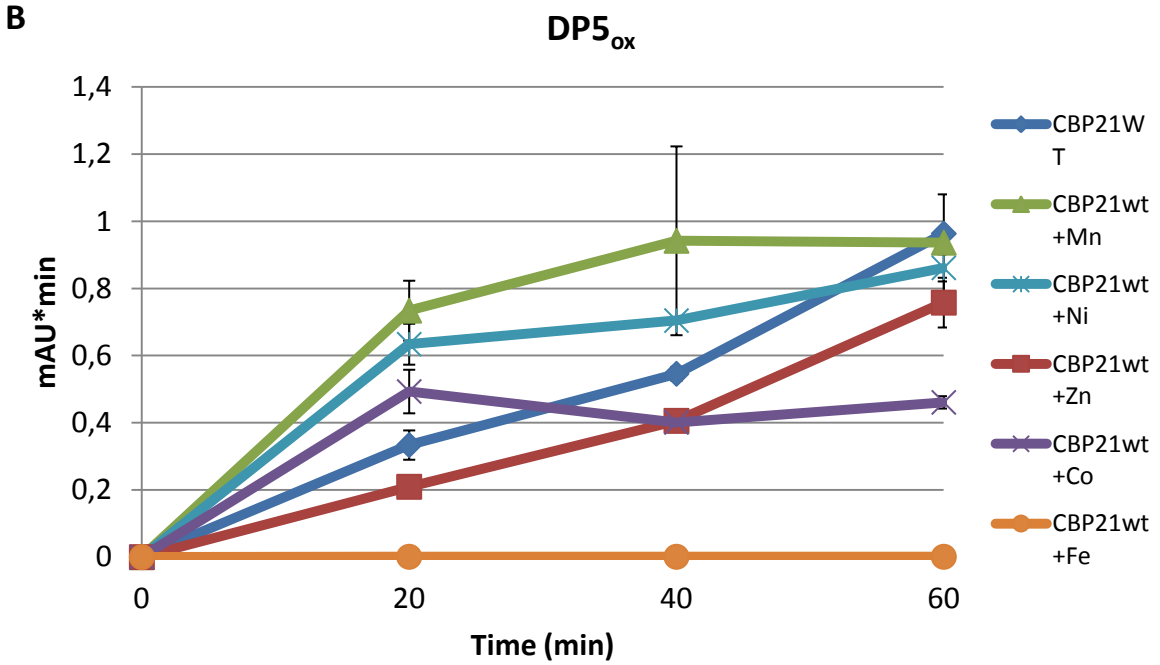

C

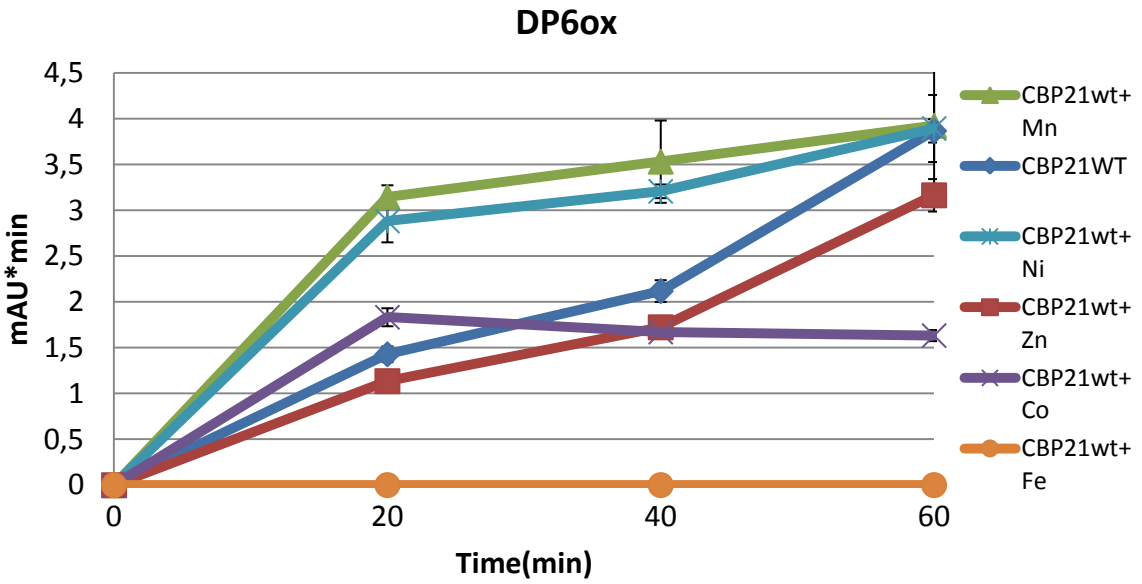
DP6ox
4,5
4
3,5
3
2,5
2
1,5
1
0,5
0
mAU*min
0
20
40
60
Time(min)
CBP21wt+ Mn
CBP21WT
CBP21wt+ Ni
CBP21wt+ Zn
CBP21wt+ Co
CBP21wt+ Fe

D

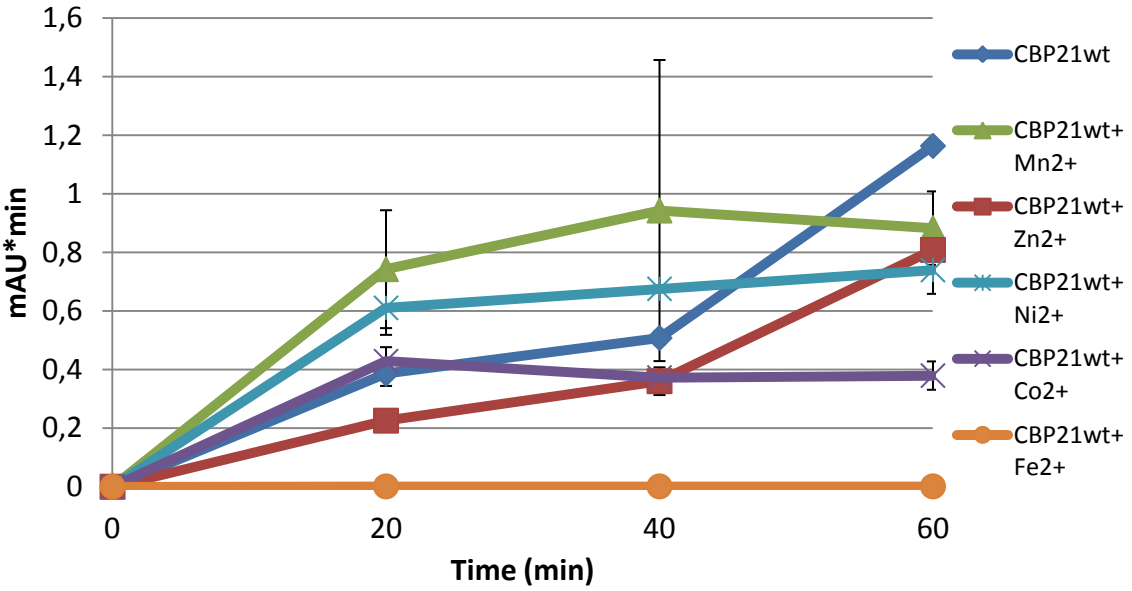
DP7ox
1,6
1,4
1,2
1
0,8
0,6
0,4
0,2
0
mAU*min
0
20
40
60
Time (min)
CBP21wt
CBP21wt+ Mn2+
CBP21wt+ Zn2+
CBP21wt+ Ni2+
CBP21wt+ Co2+
CBP21wt+ Fe2+

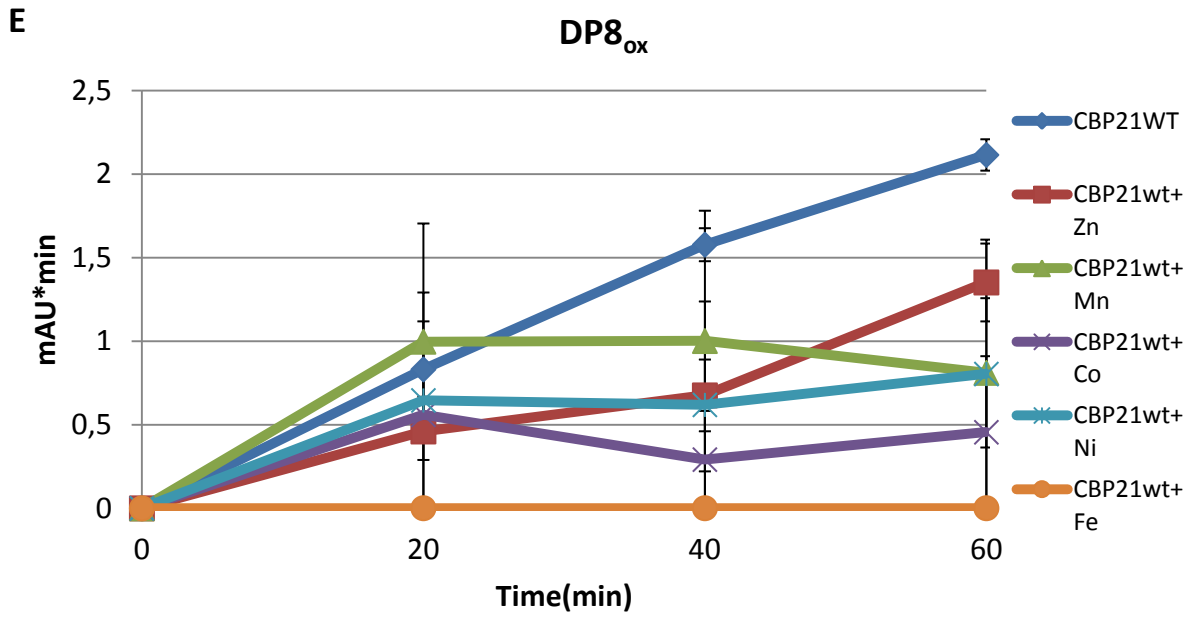

Figure. 4.7 Generation of DP_{ox} 4-8 from $CBP21_{wt}$ activity on β-chitin. Reaction mixtures contained 1µM CBP21, 2 mg/ml β-chitin, 1mM ascorbic acid in 20mM Tris-HCL buffer pH 8.0 and 5mM metal ions, except from the positive control (CBP2wt), where no metal ions were added. $CBP2_{wt}$ and the respective metal ion were preincubatet for 15 minutes in buffer solution before addition of chitin and ascorbic acid. All reactions were incubated at 37^0C and 750 rpm. Each data point represents the mean value of three replicates.

All in all, the data of Fig. 4.7 clearly show the full inhibitory effect of Fe^{3+} and further show that Mn^{2+} and Ni^{2+} after 90 minutes probably hardly affect $CBP2_{wt}$ activity, whereas Zn^{2+} reduces activity to some extent, inhibitory effect for Co^{2+} is also clear after 90 minutes. An more detailed analysis show that in the first phase (0-20) minutes Mn^{2+}, Ni^{2+} and Co^{2+} promote $CBP21_{wt}$ activity, except for DP8 products.

4.2.3 The influence of metal ions on the $CBP21_{wt}$ -chitinase synergy

The ability of the *S. marcescens* chitinase ChiC to hydrolyze β-chitin in the presence of $CBP2_{wt}$ and various divalent metal ions was analyzed by UHPLC using an ion exclusion method for separation of the main products (mono- and disaccharides) (see section 3.10.2). The detected chitooligosaccharide in this synergy experiment was the major product from chitin hydrolysis by ChiC, namely $GlcNAc_2$. The degradation rates in reactions containing metal ions are compared with the rates in a synergy experiment with $CBP21_{wt}$ and ChiC in the absence of added metal ions, where the latter reaction serves as a positive control (Figure 4.8).

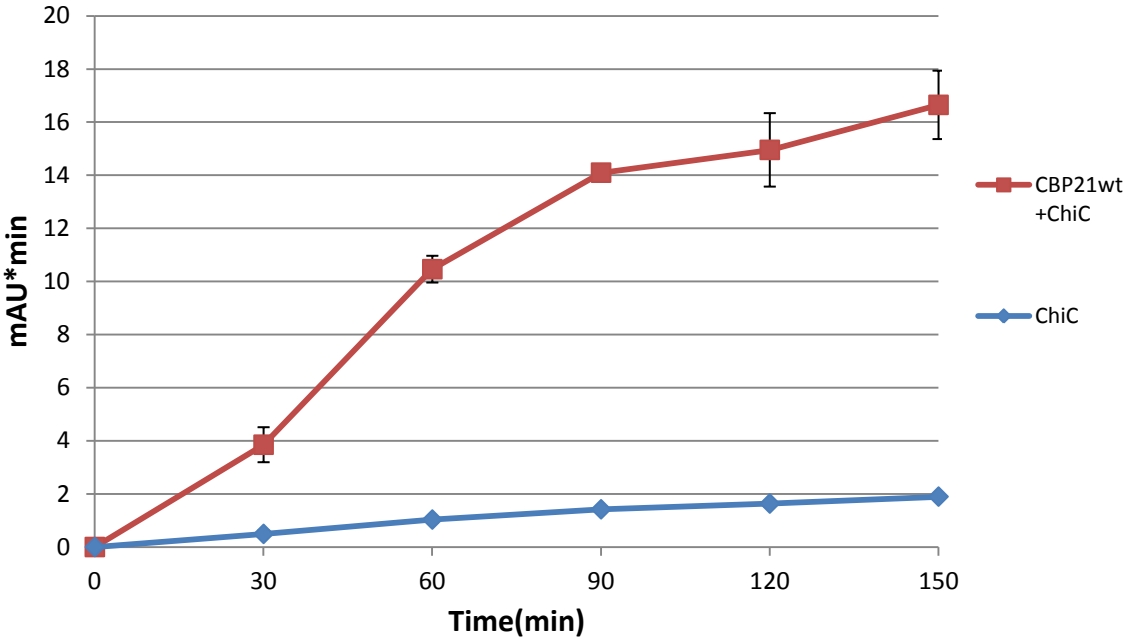

Figure 4.8 Degradation of β-chitin by ChiC in the absence and presence of $CBP21_{wt}$. The reaction $CBP21_{wt}$+ ChiC (marked with red squares) contained 1 µM $CBP21_{wt}$, 0.1 µM ChiC, 2mg/ml β-chitin and 1mM ascorbic acid. The reaction ChiC (market with blue diamonds) contained 0.1 µM ChiC , 2mg/ml β-chitin and 1mM ascorbic acid. The reactions were incubated at 37^0C and 750 rpm. Each data point represents the mean value of three replicates.

Figure 4.8 show the important contribution from $CBP21_{wt}$ upon β-chitin degradation process as it boosts chitin turnover by approximately 8 fold. When 5 mM metal ions were included in the reactions it became clear that Zn^{2+} and Co^{2+} reduced overall synergy, whereas Ni^{2+} and Mn^{2+} had barely no effects, at least for the long term degradation rate. In the reaction containing Fe^{3+} product formation was completely abolished (figure 4.9 A-E).

Notably, the effect of the metal ions varies over time. In the initial phase of the reactions (0 to 30 min) all reactions with metal ions (except Fe^{3+}) exhibited a higher rate of chitin turnover. In the second phase, after 30 minutes, the synergi activity in reactions containing Zn^{2+} and Co^{2+} were clearly reduced. At 150 minutes these reactions both showed significant less concentrations of $(GlcNAc)_2$ compared to the control reaction. For Mn^{2+} and Ni^{2+} the rate of product runover were similar to the control, and at 150 minutes both showed close to the same amount of $(GlcNAc)_2$.

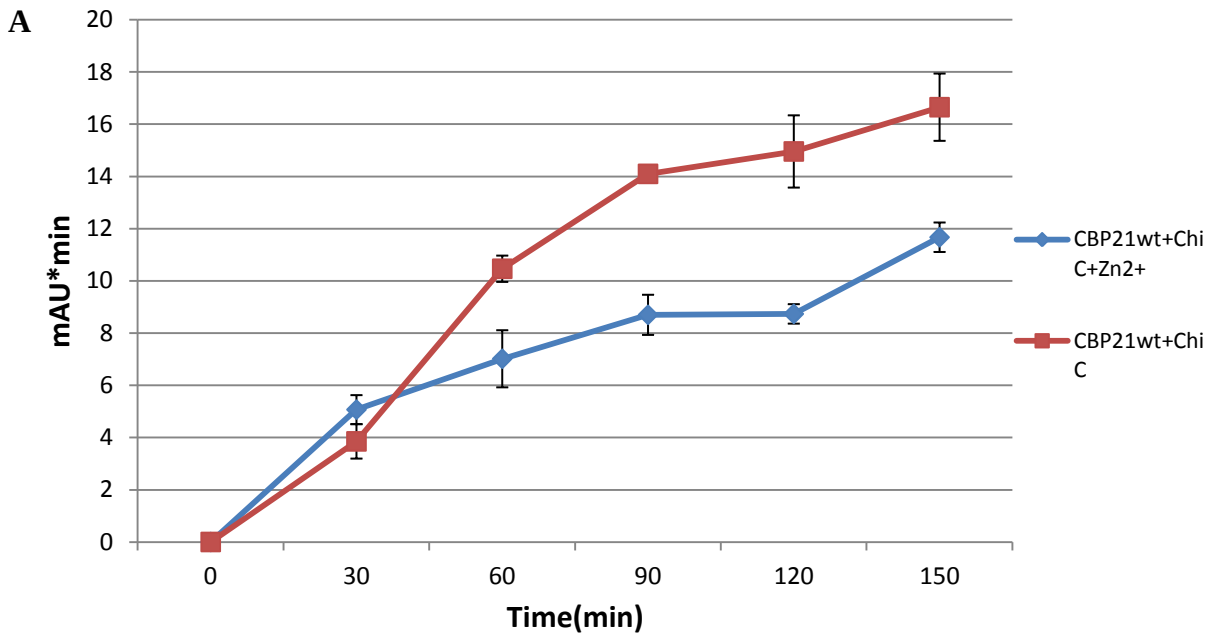

B

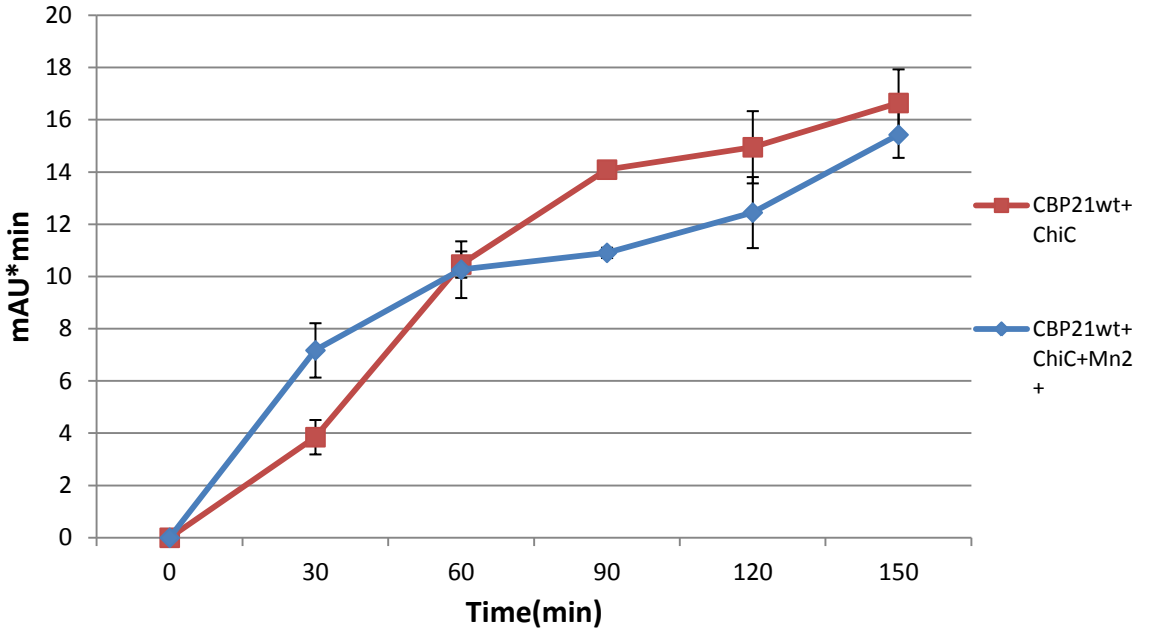
20
18
16
14
12
10
8
6
4
2
0
mAU*min
0
30
60
90
120
150
Time(min)
CBP21wt+ ChiC
CBP21wt+ ChiC+Mn2 +

C

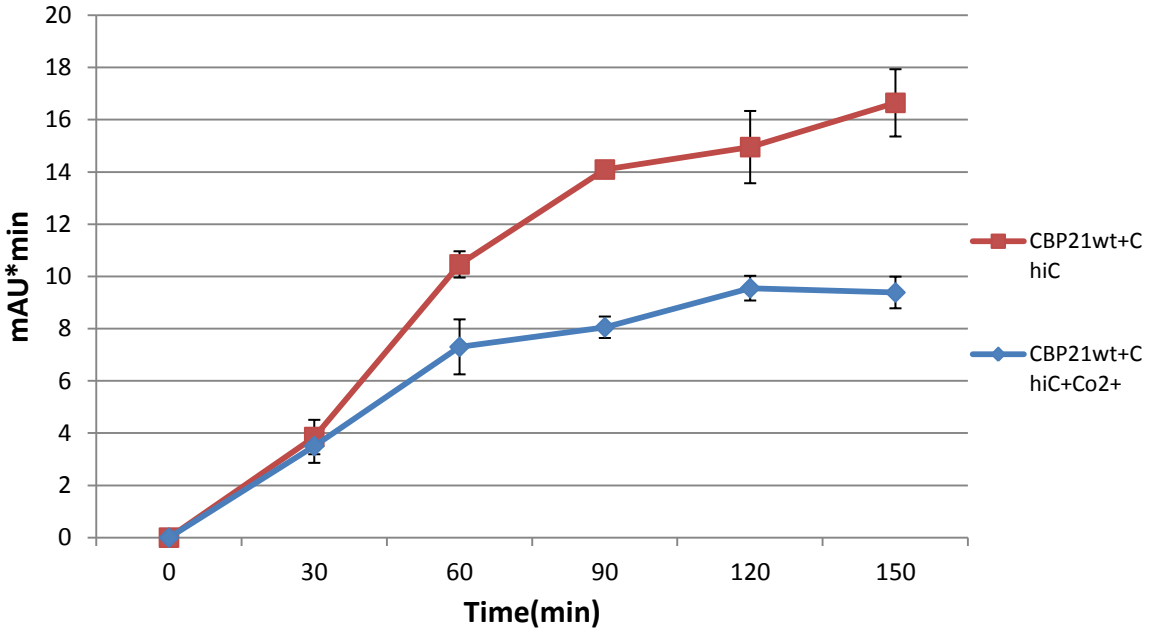
20
18
16
14
12
10
8
6
4
2
0
mAU*min
0
30
60
90
120
150
Time(min)
CBP21wt+C hiC
CBP21wt+C hiC+Co2+

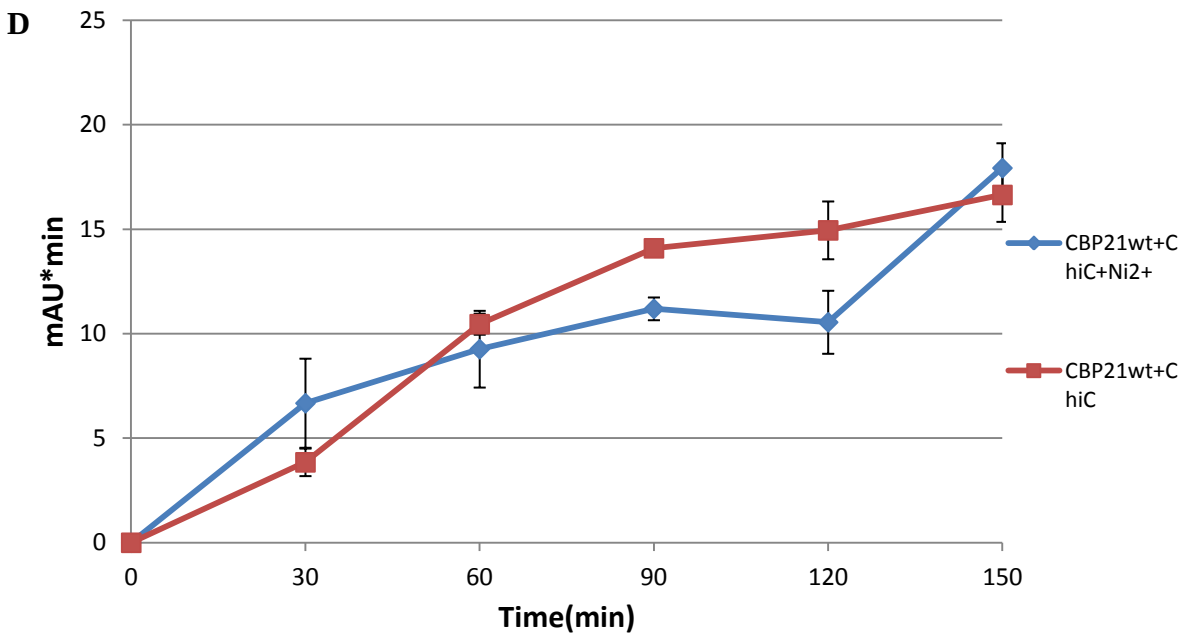

Figure 4.9 Degradation of β-chitin in synergy experiment . Reaction mixture containing 1 µM enzyme, 0.1 µM ChiC, 2mg/ml β-chitin and 1mM ascorbic acid and 5mM metal ions (120 minutes preincubaion time). CBP21 and the respective metal ion have been preincubatet for 120 minutes in buffer solution before addition of ChiC, chitin and ascorbic asid. Alls samples are incubated at 37^0C and 750 rpm. Each data point is represented from the mean value of three replicates. A, reaction with Zn^{2+} ions; B, reaction with Mn^{2+} ions; C, reaction with Co^{2+} ions; D, reaction with Ni^{2+}; E, reaction with Fe^{3+} .All figures A-E represent the generation of$(GlcNAc)_2$.

Figure 4.10 below shows a figure where all the results from the synergy assay are represented. From this figure it is clear that reactions with Mn^{2+} and Ni^{2+} shows $CBP21_{wt}$ activity comparable to the control. Inhibition from reaction with Zn^{2+} and Co^{2+} also is clear after 120 minutes. Reaction with Fe^{3+} show no enzyme activety

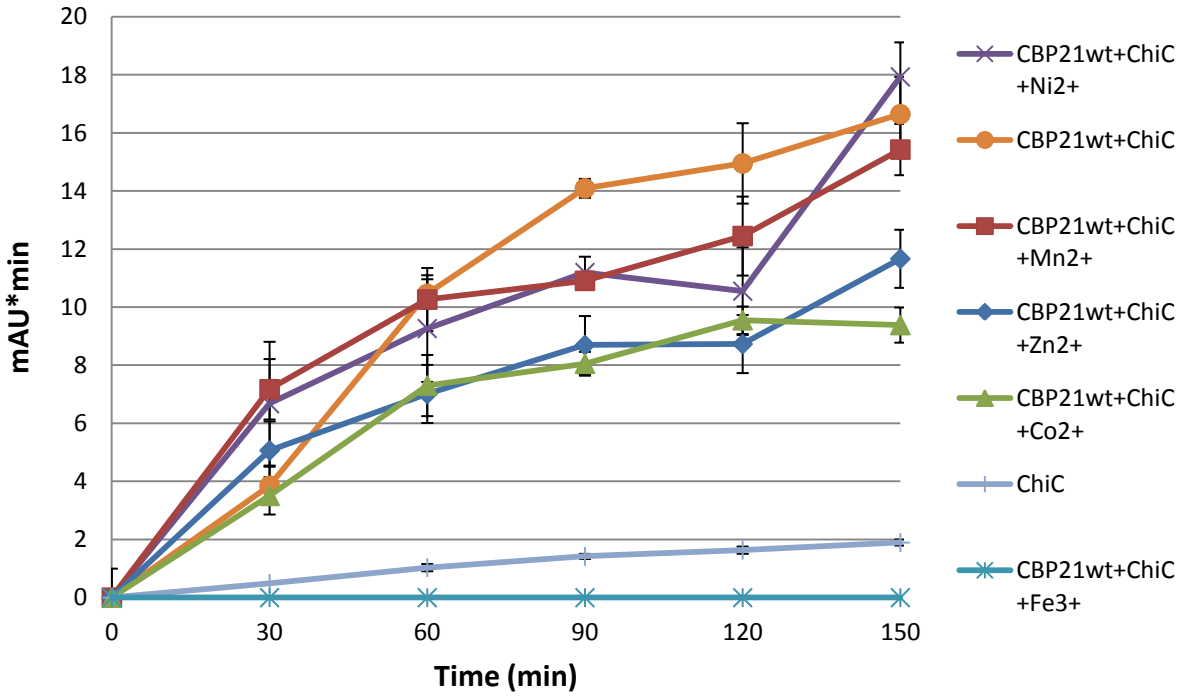

Figure 4.10 Degradation of β-chitin in synergy experiment . Reaction mixture containing 1 µM enzyme, 0.1 µM ChiC, 2mg/ml β-chitin and 1mM ascorbic acid and 5mM metal ions (120 inutes preincubaion time). CBP21 and the respective metal ion have been preincubatet for 120 minutes in buffer solution before addition of ChiC, chitin and ascorbic asid. Alls samples are incubated at 37^0C and 750 rpm. Each data point is represented from the mean value of three replicates

DISCUSION

The ability of CBP21 to bind several different metal ions in it active site, was essential inspiration towards researching the impact from metal ions on CBP21 activity.
This study is relevant as there are likely that metal ions can occur in substrate and reactors, where they may inhibit or affect activity. Especially concerns about Zn^{2+} since Aachmann et al. (2010) have shown that it could bind to CBP21 relative efficiently compared to other metals. Understanding how the enzyme activity is affected in can be useful for enzymatic biomass degradation processes.

Experiment reviling the first family AA9 (LPMO) structure showed that in the cluster of the three highly conserved histidines at the surface of the n-terminus appeared to be a metal ion binding site. The metal ion binding at this site was initially identified as magnesium(Harris et al., 2010), further experiments showed that binding site also could bind zinc ions. After initial confusion where it was postulated that LPMOs could function with a wide range of divalent metals. Aachmann et al. (2010) showed that the LPMO CBP21 in fact is copper dependent and further showed that Ca^{2+}, Mg^{2+}, Fe^{2+}, Co^{2+}, Zn^{2+} and Cu^{2+} where able to bind to the active site. The ability of CBP21 to bind different metal ions where not addressed in detailed, except for the metals Cu^{2+} and Zn^{2+}, where ITC experiment where conducted, sthat Cu^{2+} Kd values of 55 nM and Zn^{2+} 330nM(Aachmann et al., 2012).

Experimental work

In the purification process with chitin- affinity chromatogram there were experienced some problems, which led to some loss of CBP21. This is evident from the SDS-PAGE gel where the band equal to CBP21 is present in the flow trough sample from purification process. This could be caused by a low amount of column material or high flow rate which all will lead to weak interaction between the chitin and CBP21 and wash the en enzyme out. The flow trough fraction was saved in case of need for further purification, but was not necessary. The purified CBP21 was then exposed for two different separate treatments, one where there were CBP21 apo enzyme generated and one where it was saturated with Cu^{2+} following desalting. CBP21 activity is dependent on copper and therefore it is important that it is equally saturated with

copper. The apo-enzymes where never taken in use since the objective of the study changed a in the beginning. First the idea was to study CBP21 activity when bound to metals other than copper, but after considering the small possibility that the enzyme could function with other metals, a decision was made to research the impact on enzyme activity in presence of metal ions.

Generally is not straightforward to determine LPMO activity quantitatively, as the catalysis from these enzymes is located on the insoluble substrate, whereas it is the soluble product generated by the enzymes which is analyzed. Enzyme activity on the unsalable substrate will not be quantified. In addition the enzymes are unstable over time and it is not clear what the limiting factors are. Several methods were used for a systematically analysis of enzyme activity, MALDI-TOF MS for qualitative- and HPLC methods for quantitative analysis. The result which is further discussed was comparable for all methods. The decision of activity from MALDI-TOF MS analysis was done by indicating activity or no activity, meaning that if there were analyzed oxidized product it was interoperated as positive activity. Giving an more quantitative ruling of activity from MALDI-TOF MS assay showed to be difficult, because the measurements was highly dependent on the grade of crystallization, location on the spot where the laser was shoot at and laser intensity.

If CBP21 had been added to the sample it could bind to the substrate, then blocking the possibility for ion exchange in its active site. This led to the introduction of an additional parameter, which was the time that the metal ions was incubated with CBP21before addition of substrate and reducing agent, called preincubation time. This would allow additional ions to compete with the copper if possible.

The MALDI-TOF MS data showed that the fully inhibitory effect from metal ions on CBP21 was first evident at very high concentration. Fe^{3+} ions fully inhibited enzyme activity at 2mM consternations and higher. It is not likely that this is caused by a change of metal ion in the active site of CBP21 which leads to inactivation, more likely Fe^{3+} trough fenton chemistry generates hydrogen peroxide H_2O_2 which will eliminate CBP21 activity. CO^{2+} and Zn^{2+} inhibited enzyme activity first at 10 mM consecrations. For zinc ions this was first seen at 15 minutes preincubation time. It was anticipated that Zn^{2+} based on its ability to bind to CBP21 would be able to deactivate the enzyme at longer preincubation time and at lower concentrations, but this was not observed. The inhibitory effect on the enzyme at these consecrations was not tested by HPLC when it was considered to be significant higher then

what to except outside of laboratory conditions. 5 mM ion concentrations with 15 and 120 minutes preincubation time was further tested for enzyme activity by two different HPLC methods.

The quantitatively analysis from UHPLC detecting oxidized products showed that reactions with Fe^{3+} had full inhibition, comparable to MALDI-TOF experiment. Reactions with Zn^{2+} showed a relative activity close to 70-80% compared to the control. It was expected that zinc ions would bind to CBP21 and reduce activity, as the results showed. Reactions with Mn^{2+}, Ni^{2+} and Co^{2+} showed an increased activity for the first phase of the reactions in the second phase the activate tend to slow down. At 90 minutes the enzyme activity in reactions with Mn^{2+} and Ni^{2+} comparable with the control, especially for DP4 and DP6, for Co^{2+} the activity is around 40% compared to the control. Highest activity relative compared to the control was for Mn^{2+} where over a twofold in activity after 20 minutes were detected.

Analysis of the synergy experiment revealed results much similar to the UHPL analysis of oxidized products. Fe^{3+} showed 100% inhibition. Zinc ions had around 70% relative activity compared to the control. Reactions with Mn and Ni ions showed increased activity in the initial rate, but with time the activity was similar to the control. Reactions with Co^{2+} stood out by having an all over less CBP21 activity, which was a little different from what observed from the first UHPLC experiment. The second phase in reactions dident illustrates the same reduced activity as for the first UHPLC method. This can be a result that in the initial phase the $CBP21_{wt}$ are degrading the substrate at a very high level, then the enzyme most likely will have the same slower second phase observed earlier in the first UHPLC methods. But the initial activity have made enough soluble products that it will keep ChiC activity occupied throughout the reaction time. And therefore a higher turnover rate is observed in the second phase for this method.

Fe^{3+} inhibits enzyme activity for the same reasons discussed above for MALDI-TOF MS results. It is not expected that the reason for increased activety in reactions from both methods, is caused by the metal ions outcompete copper and increase the CBP21 activity. More possible explanations is that the metal ions function like a catalyst for the using the oxygen in the reaction, or the metal ions can contribute to a better flow of electrons, increasing the initial rate of the enzyme while generating H_2O_2. The fact that the enzyme activity is slowing down, support that the idée that the ions contribute to usage of the oxygen or electrons at a higher rate and generate H_2O_2. Generation of H_2O_2 will contribute to

inactivate the enzymes in the reaction. It is not possible to rule out the possibility that the enzyme could be active with the different metal ions in its active site, since there were no experiments done with CBP21 apo enzymes saturated with the different metal, followed by analysis of activity.

The conclusion is that Fe^{3+}, Zn^{2+} and Co^{2+} ions where able to inhibit CBP21 activity, at 2mM 10mM and 10mM concentrations, respectively. Zinc which is known to be able to bind to the active site of CBP21 reduced it activity by approximate 20-30% for consecrations at 5 mM. Mn^{2+} and Ni^{2+} increased the CBP21 activity special in the initial phase of the reactions but not over time. Co^{2+} did showed a slight increase in initial enzyme activity but over time it inhibited the activity. The mechanism behind the effect of the metal ions tested on CBP21 activity is not clear. Better quantitative assays are needed to gain more data on the activity of CBP21. Experiment like ITC for Mn^{2+} and Ni^{2+} could yield some informative data. For further analysis on this subject experiment with apo enzyme saturated with the different metal ions and further analysis of activity could be interesting.

Aachmann, F. L., Sorlie, M., Skjak-Braek, G., Eijsink, V. G., & Vaaje-Kolstad, G. (2012). NMR structure of a lytic polysaccharide monooxygenase provides insight into copper binding, protein dynamics, and substrate interactions. *Proc Natl Acad Sci U S A, 109*(46), 18779-18784. doi: 10.1073/pnas.1208822109

Bradford, M. M. (1976). A rapid and sensitive method for the quantitation of microgram quantities of protein utilizing the principle of protein-dye binding. *Analytical biochemistry, 72*(1), 248-254.

Cantarel, B. L., Coutinho, P. M., Rancurel, C., Bernard, T., Lombard, V., & Henrissat, B. (2009). The Carbohydrate-Active EnZymes database (CAZy): an expert resource for Glycogenomics. *Nucleic Acids Res, 37*(Database issue), D233-238. doi: 10.1093/nar/gkn663

Carlström, D. (1957). The crystal structure of α-chitin (poly-N-acetyl-D-glucosamine). *The Journal of biophysical and biochemical cytology, 3*(5), 669-683.

Eijsink, V. G., Vaaje-Kolstad, G., Vårum, K. M., & Horn, S. J. (2008). Towards new enzymes for biofuels: lessons from chitinase research. *Trends in biotechnology, 26*(5), 228-235.

Forsberg, Z., Vaaje-Kolstad, G., Westereng, B., Bunaes, A. C., Stenstrom, Y., MacKenzie, A., . . . Eijsink, V. G. (2011). Cleavage of cellulose by a CBM33 protein. *Protein Sci, 20*(9), 1479-1483. doi: 10.1002/pro.689

Fuchs, R., McPherson, S., & Drahos, D. (1986). Cloning of a Serratia marcescens gene encoding chitinase. *Applied and environmental microbiology, 51*(3), 504-509.

Gardner, K., & Blackwell, J. (1975). Refinement of the structure of β-chitin. *Biopolymers, 14*(8), 1581-1595.

Giraud-Guille, M., & Bouligand, Y. (1986). Chitin-protein molecular organization in arthropod *Chitin in Nature and Technology* (pp. 29-35): Springer.

Gooday, G. W. (1990). The ecology of chitin degradation *Advances in microbial ecology* (pp. 387-430): Springer.

Harding, S. E., & Adams, G. G. (2002). *An Introduction to Polysaccharide Biotechnology*: Taylor & Francis.

Harris, P. V., Welner, D., McFarland, K., Re, E., Navarro Poulsen, J.-C., Brown, K., . . . Merino, S. (2010). Stimulation of lignocellulosic biomass hydrolysis by proteins of glycoside hydrolase family 61: structure and function of a large, enigmatic family. *Biochemistry, 49*(15), 3305-3316.

Hejazi, A., & Falkiner, F. (1997). Serratia marcescens. *Journal of Medical Microbiology, 46*(11), 903-912.

Hemsworth, G. R., Taylor, E. J., Kim, R. Q., Gregory, R. C., Lewis, S. J., Turkenburg, J. P., . . . Walton, P. H. (2013). The copper active site of CBM33 polysaccharide oxygenases. *Journal of the American Chemical Society, 135*(16), 6069-6077.

Hoell, I. A., Vaaje-Kolstad, G., & Eijsink, V. G. (2010). Structure and function of enzymes acting on chitin and chitosan. *Biotechnology and Genetic Engineering Reviews, 27*(1), 331-366.

Horn, S. J., Sorbotten, A., Synstad, B., Sikorski, P., Sorlie, M., Varum, K. M., & Eijsink, V. G. (2006). Endo/exo mechanism and processivity of family 18 chitinases produced by Serratia marcescens. *FEBS J, 273*(3), 491-503. doi: 10.1111/j.1742-4658.2005.05079.x

Horn, S. J., Vaaje-Kolstad, G., Westereng, B., & Eijsink, V. G. (2012). Novel enzymes for the degradation of cellulose. *Biotechnol Biofuels, 5*(1), 1-13.

Jang, M. K., Kong, B. G., Jeong, Y. I., Lee, C. H., & Nah, J. W. (2004). Physicochemical characterization of α-chitin, β-chitin, and γ-chitin separated from natural resources. *Journal of Polymer Science Part A: Polymer Chemistry, 42*(14), 3423-3432.

Jee, J.-G., Ikegami, T., Hashimoto, M., Kawabata, T., Ikeguchi, M., Watanabe, T., & Shirakawa, M. (2002). Solution Structure of the Fibronectin Type III Domain fromBacillus circulans WL-12 Chitinase A1. *Journal of Biological Chemistry, 277*(2), 1388-1397.

Levasseur, A., Drula, E., Lombard, V., Coutinho, P. M., & Henrissat, B. (2013). Expansion of the enzymatic repertoire of the CAZy database to integrate auxiliary redox enzymes. *Biotechnol Biofuels, 6*(1), 41. doi: 10.1186/1754-6834-6-41

Minke, R., & Blackwell, J. (1978). The structure of α-chitin. *Journal of molecular biology, 120*(2), 167-181.

Monreal, J., & Reese, E. T. (1969). The chitinase of Serratia marcescens. *Canadian Journal of Microbiology, 15*(7), 689-696.

Pace, C. N., Vajdos, F., Fee, L., Grimsley, G., & Gray, T. (1995). How to measure and predict the molar absorption coefficient of a protein. *Protein science, 4*(11), 2411-2423.

Perrakis, A., Tews, I., Dauter, Z., Oppenheim, A. B., Chet, I., Wilson, K. S., & Vorgias, C. E. (1994). Crystal structure of a bacterial chitinase at 2.3 Å resolution. *Structure, 2*(12), 1169-1180.

Phillips, C. M., Beeson, W. T., Cate, J. H., & Marletta, M. A. (2011). Cellobiose dehydrogenase and a copper-dependent polysaccharide monooxygenase potentiate cellulose degradation by Neurospora crassa. *ACS Chem Biol, 6*(12), 1399-1406. doi: 10.1021/cb200351y

Rinaudo, M. (2006). Chitin and chitosan: properties and applications. *Progress in polymer science, 31*(7), 603-632.

Rudall, K., & Kenchington, W. (1973). The chitin system. *Biological Reviews, 48*(4), 597-633.

Suzuki, K., Suzuki, M., Taiyoji, M., Nikaidou, N., & Watanabe, T. (1998). Chitin binding protein (CBP21) in the culture supernatant of Serratia marcescens 2170.

Vaaje-Kolstad, G., Horn, S. J., Sorlie, M., & Eijsink, V. G. (2013). The chitinolytic machinery of Serratia marcescens--a model system for enzymatic degradation of recalcitrant polysaccharides. *FEBS J, 280*(13), 3028-3049. doi: 10.1111/febs.12181

Vaaje-Kolstad, G., Horn, S. J., van Aalten, D. M., Synstad, B., & Eijsink, V. G. (2005). The non-catalytic chitin-binding protein CBP21 from Serratia marcescens is essential for chitin degradation. *J Biol Chem, 280*(31), 28492-28497. doi: 10.1074/jbc.M504468200

Vaaje-Kolstad, G., Houston, D. R., Riemen, A. H., Eijsink, V. G., & van Aalten, D. M. (2005). Crystal structure and binding properties of the Serratia marcescens chitin-binding protein CBP21. *J Biol Chem, 280*(12), 11313-11319. doi: 10.1074/jbc.M407175200

Vaaje-Kolstad, G., Westereng, B., Horn, S. J., Liu, Z., Zhai, H., Sorlie, M., & Eijsink, V. G. (2010). An oxidative enzyme boosting the enzymatic conversion of recalcitrant polysaccharides. *Science, 330*(6001), 219-222. doi: 10.1126/science.1192231

Watanabe, T., Kimura, K., Sumiya, T., Nikaidou, N., Suzuki, K., Suzuki, M., . . . Regue, M. (1997). Genetic analysis of the chitinase system of Serratia marcescens 2170. *Journal of bacteriology, 179*(22), 7111-7117.

Westereng, B., Ishida, T., Vaaje-Kolstad, G., Wu, M., Eijsink, V. G., Igarashi, K., . . . Sandgren, M. (2011). The putative endoglucanase PcGH61D from Phanerochaete chrysosporium is a metal-dependent oxidative enzyme that cleaves cellulose. *PLoS One, 6*(11), e27807. doi: 10.1371/journal.pone.0027807

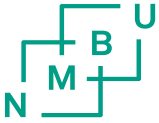

Norwegian University
of Life Sciences

Postboks 5003
NO-1432 Ås, Norway
+47 67 23 00 00
www.nmbu.no